Metrological features of the Large Piston Prover at INRIM

Measurement

Metrological features of the Large Piston Prover at INRIM

--Manuscript Draft--

Manuscript Number:	MEAS-D-21-05579R2
Article Type:	Research Paper
Keywords:	primary flow standard; volumetric calibration; uncertainty analysis; test rig development; flow calibration
Corresponding Author:	Pier Giorgio Spazzini, PhD INRIM: Istituto Nazionale di Ricerca Metrologica Torino, ---- ITALY
First Author:	Aline Piccato, PhD
Order of Authors:	Aline Piccato, PhD
	Marco Bisi, PhD
	Pier Giorgio Spazzini, PhD
	Fabio Bertiglia
	Gaetano La Piana
	Emanuele Audrito
	Marco Santiano
	Roberto Bellotti
	Claudio Francese
Abstract:	INRIM realizes its flow rate standard using three facilities with different flow rate ranges; in particular, the largest flow range (10-2600 L/min) is obtained through a piston prover (nominal diameter 1000 mm and nominal stroke 1200 mm). This is a volumetric type machine, therefore its traceability is obtained through dimensional calibration. The paper describes the features of the standard, its traceability chain and its uncertainty budget, which directly determines the associated Calibration and Measurement Capabilities claim. A detailed analysis of the uncertainty components will be presented, paying special attention to the dimensional calibration of the piston. This calibration is particularly challenging due to the large size of the piston, which requires in-situ calibration and thereby special adaptations with respect to the standard calibration of a cylinder. The calibration here discussed is in good accordance with the one carried on in 1999, thus confirming the stability of the standard.

Cover letter

Torino (Italy), November 9, 2021

Editorial Department of Measurement

Dear Editor of Measurement,

I am submitting a manuscript for consideration of publication in Your Journal. The manuscript is entitled “Metrological features of the Large Piston Prover at INRIM”.
It has not been published before, although it was previously submitted to “Metrologia”, from which it was rejected since it was deemed as outside the scopes of the journal. We also received some suggestions for improvement, which were included in the present version.
The paper presents a detailed description of the geometrical calibration of a test rig used for accurate flow measurement, alongside with a full evaluation of the uncertainty of the flow generated by the test rig; the authors believe that it can be of interest in the framework of defining the state of the art in the field of traceable measurement of flow rates, with special focus on the uncertainty estimation. In particular, the approach used for the uncertainty budget could be of interest to suggest a very specific approach in this metrological field. Therefore, the authors believe that this paper could be of interest for NMIs or DIs in developing a primary gas flow standard.

Thank you very much for your consideration.

Yours Sincerely,

Pier Giorgio Spazzini, PhD (on behalf of all the Authors)

Applied Metrology and Engineering Division, INRIM

Strada delle Cacce, 91 – I10137 Torino (Italy)

Tel.: +39 (0)11 3919941

E-mail: p.spazzini@inrim.it

- Calibration of a Piston Prover for accurate flow rate measurement;
- Analysis of volumetric measurements on a large piston;
- Detailed uncertainty analysis of a primary flow test rig;
- Uncertainty budget with determination of main contributions.

Ms. Ref. No.: MEAS-D-21-05579R1

Reviewers' comments:

Reviewer #3:

Comments:
Referring to questions numbered in the first revision and authors'answers,

(1) It is not necessarily correct to say that direct mass flowrate measurement is better (smaller uncertainty) than indirect mass flow measurement obtained by the volumetric displacement of the piston prover. The authors should demonstrate it by comparisons with the results of an alternative available design, or simply suppress this statement.

ANSWER: The statement was suppressed and replaced by simply stating that the use of this method is a choice of our laboratory, alongside with the explanation of the points that determined our choice (see par. 3).

(2) Non uniformities are usually dealt as type B uncertainty evaluation, unless a better procedure is used. The authors should give enough information so that the uncertainty can be estimated properly.

ANSWER: We reformulated par. 4.3.2 to better explain the procedure for the evaluation of temperature non uniformities, which are actually evaluated at every measurement (we realized that we wrote “periodically checked”, that was a typo). We think that the evaluation of the uncertainty associated to non uniformities by evaluation of the standard deviation of the outputs from a relatively large number of probes should be an appropriate estimate.

(3)If there is a leakage through the gap between the piston and the wall, the volumetric gas flowrate is not the same as the volumetric displacement of the piston prover. The authors should refer to earlier studies (could be an internal report) , or simply state the no leakage assumption as hypothesis.

ANSWER: the gap between the piston and the wall is free, the seal of the chamber is guaranteed by the gasket at the top of the cylinder as described in Par. 2.2; of course leaks are a big concern, and we check them periodically as described in Par. 4.3.7.

(4) Accepted.

ANSWER: OK.

(5) The authors should refer to a reference (or even an internal report) to justify the existence of a covariance term.

ANSWER: Since pressure and temperature measurements are performed using the same instruments at the beginning and at the end of the test run, these measurements are correlated and therefore there is a covariance term, as specified in the document “JCGM 100:2008 GUM 1995 with minor corrections”, par. F.1.2.3 (page 62).

(6) The authors should calculate the compressibility factor of the gas to demonstrate that the error in considering the ideal gas law has a small influence for estimating the uncertainty of flowrate measurement.

ANSWER: We added par. 4.3.8 to take into account the Reviewer’s comment.

(7) Accepted.

ANSWER: OK.

(7) Accepted.

ANSWER: OK.

Metrological features of the Large Piston Prover at INRIM

Abstract

INRIM realizes its flow rate standard using three distinct facilities, aimed at measuring different flow rate ranges; in particular, for the largest flow range rate (10-2600 L/min) a piston prover is used. This machine is of the volumetric type, therefore its traceability can be obtained through dimensional calibration of the piston, which has a nominal diameter of 1000 mm and a nominal stroke of 1200 mm.

The present paper describes in detail the features of the standard, its traceability chain and the uncertainty budget of the measurements it can perform. The uncertainty budget directly determines the Calibration and Measurement Capabilities claim in the range available to the test rig. A detailed analysis of the various uncertainty components will be presented and discussed. Special attention will be dedicated to the dimensional calibration of the piston, since it is of paramount importance for the determination of the main uncertainty component. This calibration is particularly challenging since, due to the large size of the piston, it must be carried on in-situ, thereby requiring a set of special adaptations with respect to a standard calibration of a cylinder. It will be shown that the calibration of the piston recently performed is in good accordance with the one that was carried out at the piston initial installation in 1999, thus confirming the stability of the standard.

Keywords

primary flow standard; volumetric calibration; uncertainty analysis; test rig development; flow calibration

1. Introduction

Accurate measurement of gas flow rate is a field whose importance is well established due to the wide range of application where such quantity is of paramount importance (*e.g.* fuel gas exchange, process gas measurement in applications connected to medical/chemical industry, etc.); presently, there is a growing need for accurate calibration of mass flow meters with various Full Scale Range (FSR), that have an increasingly wide field of application (*e.g.* for dynamical gas mixing, aerospace applications, etc.). The flow rates of interest range from fractions of cubic millimeters per second to several hundreds of liters per second. For such a range of flow rates, a robust and reliable measurement technology is the piston prover volumetric method, since it provides a carefully controlled flow of gas; its accurate measurement requires a reliable and precise knowledge of the relationship between delivered volume and

piston movement, the possibility to precisely measure the gas temperature and pressure, and the possibility of using high purity gases for the tests. INRIM operates two piston provers (in addition to a bell prover) to realize the Italian National Standard of gas flow rate. Specifically, one of the pistons is dedicated to extremely low flow rates (from ≈ 0.1 Cubic Centimeters per minute – CCM to ≈ 1.2 Liters per minute) and will not be discussed here. The piston which is the subject of the present paper is the bigger one, called MeGas, which generates flows ranging from ≈ 1 Liter per minute to ≈ 2500 Liters per minute, although the higher flow rate is usually self-limited to about 1000 Liters per minute. INRIM has operated the MeGas piston prover for several years now [1]; its features include a very accurate piston machining, reduced movement friction, accurate measurement of the piston movement and of the gas thermodynamic conditions, and temperature stabilization of the environment. Although all of these features are of great importance and allow the improvement of the measurement accuracy, the main requirement for obtaining high precision measurement is still an accurate calibration of the volume of the piston. In this paper a full uncertainty budget of the test rig and the methods for determining the various uncertainty contributions will be described in detail, alongside with some considerations on the implications of such a budget for the future developments of the machine.

The piston prover concept has been used for a long time now; One of the first well-documented developments of a piston prover for use as a primary standard can be found in [2], where the adaptation of a piston prover built for liquid measurements to gas measurements is described. Since then, several variants and adaptations have been developed for various applications. A recent review of piston provers used as primary standards can be found in [3], alongside with a description of their theory of operation. In [4] a large, hydraulically-driven piston prover is described, including a discussion on the dimensional analysis of the piston itself. [5] discuss the double-piston concept, which has the advantage of allowing measurements during both runs of the piston, but at the price of an increase in complexity.

In order to provide a reference frame for the present work, the metrological properties of a few test rigs developed in other NMIs, taken from the BIPM KCDB, are presented in the following Table 1:

NMI	Standard type	Range /m^3/h	Uncertainty / %
INRIM	Piston (standard described here)	1-150	0.05
INRIM	Bell	0.06-6	0.12
VSL	Bell	1-400	0.09
VSL	Piston (see also [4])	5-230	0.06 to 0.29
CMI	Bell	0.5-280	0.07

Table 1. Metrological properties of some gas flow primary standard.

This is the third INRIM work ([6], [7]) in a series of papers that aim to disseminate the knowledge of flow measurement standards focusing on a metrological point of view. Authors think that the hypotheses and the theories underlying the uncertainty budget of a standard are fundamental for the correct evaluation of its uncertainties, but often the details of this analysis are reported in languages other than English or in laboratory procedures and technical reports which are not open access. The theoretical work of uncertainty analysis must always precede the results of international comparisons which must be limited to support the validity of detailed uncertainty evaluations. It is the authors' opinion that sharing and comparing also the theoretical evaluation of the uncertainty and not only the numerical results is important. This paper has been divided in sections in order to facilitate its reading and make the analysis even clearer and therefore usable by those who do not yet have solid experience in the field of primary standards.

2. Facility and instrumentation description

2.1. The Measurement ambient

The MeGas facility is located at the gas flow laboratory in INRIM. The laboratory is temperature controlled and the temperature during calibration can be set in the range from 15 °C to 25 °C. Whenever the temperature setting is changed, at least 12 hours should be waited before taking measurements. Under normal conditions, the temperature is set to 20 °C. The relative humidity value is currently not controlled but is measured and recorded using a TESTO thermo-hygrometer data logger. The ambient pressure too is not controlled and it is determined,

with small variations, by the external atmospheric pressure and is measured by a Ruska barometer. During a single measure of a calibration, the pressure changes must be contained within ±200 Pa. If this condition is not met, the calibration is considered invalid and repeated.

2.2. The Piston Prover

The MeGas test rig described in the present paper, is a single-stroke, plunger-type piston prover. It was designed and built at the then-IMGC (now INRIM) in the mid-1980s with the aim of developing the largest piston prover that could be housed in the existing laboratory premises. The goal of the development was the reduction of one order of magnitude of the "purely volumetric" uncertainty components that affect bell provers. This was obtained by eliminating the oil bath and by adopting a rigid, precisely machined and measured body to sweep the volume, which naturally leads to the piston prover concept. The plunger type (namely a long, vertical cylindrical piston forced to sink through a gasket into a slightly larger, rigid but mechanically unfinished chamber containing the gas) was preferred over a traditional piston-cylinder system because of metrological (the external diameter can be measured more accurately than the internal one) and practical reasons (it is easier and cheaper to machine the piston than the cylinder, and the gasket is more easily accessible).

The resulting device is a structure 6 m high (Fig. 1), with at its top a platform (Fig. 1A) where a finely controlled brushless motor drives, through a gearbox, the female ball-screw of a lead screw (Fig. 1B) connected with the piston. This apparatus causes the vertical movement of the piston (Fig. 1C) and the emission of pulses from a rotating encoder (Fig. 1A) fitted on the female screw. The piston is constituted by a 1000 mm nominal diameter, 1630 mm long and 14 mm thick carbon-steel cylinder fitted to a massive bottom flange. The external surface of the cylinder is chromium plated, ground and polished. The leak-proof gasket at the top of the chamber is a Teflon-coated, 1000 mm diameter O-ring compressed to the necessary and adjustable extent by an upper flange. The internal diameter of the measurement chamber (Fig. 1D) is 1095 mm; in the clearance between its walls and the piston, 10 Platinum Resistance Temperatures (PRTs) are installed at different heights and positions in order to measure the average gas temperature and to detect possible non uniformities. The chamber rests on the 1950 mm diameter base of the prover. A bended pipe is connected to a 100 mm bore at the center of the base which conveys the gas displaced by the piston towards the test line. A group of automatically operated valves (a safety valve, one for admission of atmospheric air and one

for gas delivery to the test line) are installed at the facility exit (Fig. 1E) . The internal volume of the prover is about 1500 L when the piston is at its upper rest position; the volume of the piston is more than 1200 L, however, considering the parts of the piston stroke that must be devoted to acceleration, deceleration and the emergency stop switches installed at both ends, the largest gas volume that can be displaced and measured is about 800 L.

2.2.1 Mode of Operation

The operation of the prover is fully automated and controlled by a specific electronic apparatus, which controls the movement according to the required mode. The instrumentation – namely the encoder, the chronometer, the various transducers measuring piston velocity, displaced volume, temperatures and pressure - is interfaced to a PC for recording of the data.

The mode of operation of the piston is as follows. The piston is placed at its initial position (top or bottom depending whether supply or admission mode is required). A period of one minute is allowed for temperature stabilization, then the piston is moved at the programmed speed. After velocity and pressure stabilize, the measurement phase begins, *i.e.* the initial measurement conditions (position of the piston y_i and thermodynamic conditions p_i, T_i) are recorded, while the chronometer is started. Once the required displacement has been performed, the final measurement conditions (position of the piston y_f and thermodynamic conditions p_f, T_f) are recorded and the chronometer is stopped, providing the test time Δt; the piston is then brought to rest. The difference $\Delta y = y_f - y_i$ between the initial and final positions of the piston is the measured displacement of the piston and, when multiplied by the piston base area (which is considered as a constant, see Sec. 4), allows the computation of the displaced volume of gas ΔV. The initial and final thermodynamics conditions allow to compute the initial and final gas densities, which are used to determine the reference volume and, together with the elapsed time, the reference flow rate provided by the piston, as described in detail in Sec. 3. Depending on the working mode, supply or admission, the sign of Δy will be different; this will lead to slightly different corrections in the determination of the final values, as described in Sec. 3. It is important to notice that measurements are taken after the stabilization of the piston movement and of the pressure, *i.e.* in stationary conditions. No unsteady effects are therefore taken into account.

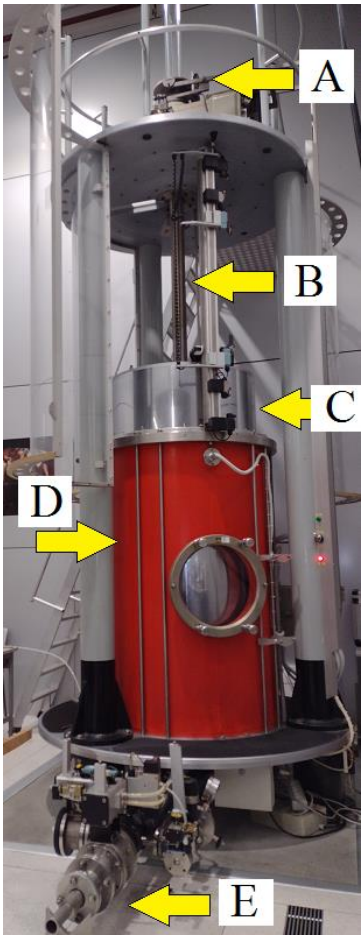

Fig. 1. MeGas Facility, A: MeGas encoder and piston control, B: screw, C: Piston, D: measurement chamber, E: facility exit

2.3. The measurement system

The traceability of the measurements carried out in the gas flow laboratory is guaranteed by the metrological chain detailed in the following traceability diagram (Fig. 2).

The traceability of the piston displacement and of the piston base area are obtained by means of the geometrical calibration of MeGas.

The traceability of the thermometric chain, the barometer and the hygrometer is guaranteed by calibration to the respective primary standards at INRIM.

Traceability of the chronometer is to the Italian National Time, as described in detail in Sec. 4.3.4.

Since this section focuses on the measurement system of the MeGas, it is important to specify that the measurement chain of MeGas during its functioning as primary standard (Sec. 2.2) does not correspond to the measurement chain used for the MeGas geometrical calibration (Sec. 4.1).

The measurement chain of the geometrical calibration of MeGas is shown in Fig. 5. During the MeGas geometrical calibration, the displacement was evaluated by an interferometric system, traceable to the INRIM primary length standard whereas the piston base area was evaluated by a couple of linear encoders that measured the diameter of the piston at different heights. The two linear encoders are traceable to the primary standard of length by calibration at INRIM.

A special, stainless steel bar traceable to the LNE primary length standard was used as reference for the linear encoders during the MeGas calibration.

The geometrical calibration of the MeGas was described in detail by three previous works [8], [9], [11]. In Sec. 4 a brief description of the geometrical calibration procedure of the MeGas is summarized in order to provide the reader with the basic elements to better understand the uncertainty analysis and the uncertainty budget.

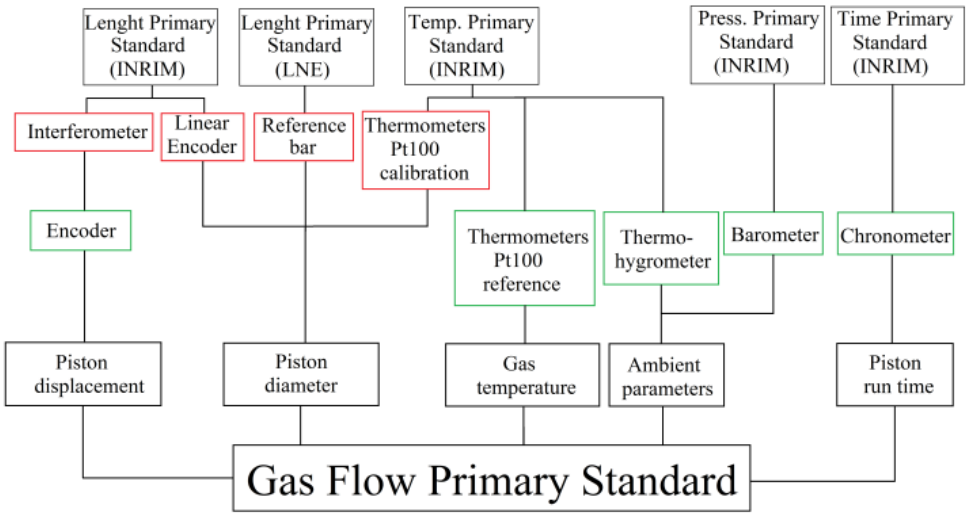

Fig. 2. Traceability diagram of MeGas. The instruments framed in red (first level line) added to the instruments framed in green (second level line) constitute the measurement chain for the MeGas calibration procedure. The instruments framed in green also constitute the in-use measurement chain of the test rig.

3. Model equation for the flow standard at MeGas

The computation of the reference volume and of the flow rate provided by the piston is done using the so-called method of the balance of mass, *i.e.* by evaluating the mass of gas delivered (or accepted) by the prover during the test. It was chosen to use this method instead of the simple determination of the volume since it allows to keep directly in consideration the variations in thermodynamic conditions for the computation of the quantity of gas that has flown through the test rig bore; additionally, the result is invariant with the thermodynamic conditions, and can therefore be readily converted to any desired form (*e.g.* molar flow, volume flow of gas at reference condition etc.); finally, the method takes directly into account the effects of compression of the dead volume, which are anyway very small due to the small overpressures within the cylinder. In Sec. 4.3.3 and 5, it will also be shown that the uncertainty associated with the measurement can be controlled with relative ease by the application of this method. The drawback of the method is that it requires measuring the initial and final thermodynamic conditions of the gas; such measurements are described in detail in Sec. 4.3.1 and 4.3.2. The displaced mass of gas ΔM is then computed as the difference between the final mass (obtained by multiplying the final density times the final volume estimate) and the initial mass (obtained by multiplying the initial density by the initial volume estimate); this difference can be rewritten as the final density by multiplying the displaced volume ΔV, computed as described in Sec. 2.2.1, with the final density and by adding a correction term which depends on the density variation and on the initial volume:

$$\Delta M = \rho_2 V_2 - \rho_1 V_1 = \rho_2 \Delta V + V_1 (\rho_2 - \rho_1) \quad (1)$$

This formulation of the equation shows that the uncertainty contribution of the initial volume is minimal (since it multiplies a value that is very small if the variation of thermodynamic conditions is small) and therefore even large uncertainties on the initial volume will affect only slightly the final result; in other words, it is not necessary to estimate the dead volume to a great accuracy, which is often difficult. ΔM can then be converted to the reference volume ΔV_{Ref} of gas – not to be confused with the displaced volume ΔV - at the specified reference conditions (which can be defined to a standard value, *e.g.* 0° C and 1 atm, or be the conditions at the Device Under Test - DUT) for comparison to the DUT output as follows:

$$\Delta V_{Ref} = \frac{\rho_2 V_2 - \rho_1 V_1}{M_{mol}} \cdot \frac{R T_{ref}}{p_{ref}} = \frac{\rho_2 \Delta V + V_1 (\rho_2 - \rho_1)}{M_{mol}} \cdot \frac{R T_{ref}}{p_{ref}} \quad (2)$$

where R is the universal gas constant, M_{mol} is the molar mass of the test gas, T_{ref} and p_{ref} are the thermodynamics conditions to be used for the conversion.

It should be noted that in writing Eq. 1 it is assumed that the final volume is larger than the initial one (admission mode) in order to have a positive value of the mass variation and therefore of the reference volume. The corresponding equation for supply mode is slightly different in that signs are opposite; this leads to small changes in the final formulation used for the computations, but the analysis of this second formulation can be performed in the same way leading to similar results (not presented here for conciseness).

The flow rate, in mass (Q_M) or volume (Q_V), is computed by dividing the computed mass or volume by test time measured by the chronometer:

$$Q_M = \frac{\rho_2 V_2 - \rho_1 V_1}{\Delta t} = \frac{\rho_2 \Delta V + V_1 (\rho_2 - \rho_1)}{\Delta t} \quad (3a)$$

$$Q_V = \frac{\rho_2 V_2 - \rho_1 V_1}{t \cdot M_{mol}} \cdot \frac{R T_{ref}}{p_{ref}} = \frac{\rho_2 \Delta V + V_1 (\rho_2 - \rho_1)}{t \cdot M_{mol}} \cdot \frac{R T_{ref}}{p_{ref}} \quad (3b)$$

Eq. 3a and Eq. 3b represent the formulation of the model equations for the computation of the flow rate delivered or accepted by the prover, while Eq. 2 is the formulation for the computation of the reference volume delivered or accepted by the prover. In the following the uncertainty analysis will be performed starting from Eq. 3b, since the corresponding analysis for Eq. 2 and Eq. 3a can readily be obtained by elimination of some terms.

4. Uncertainty analysis

The uncertainty analysis will be performed according to the document JCGM 100:2008 [10] based on Eq. 3b. The latter can be rewritten as:

$$Q_V = \frac{\Delta M}{t \cdot M_{mol}} \cdot \frac{R T_{ref}}{p_{ref}} \quad (4)$$

Eq. 4 is a multiplicative model, therefore the uncertainty associated to it can readily be obtained as:

$$\frac{u^2(Q_V)}{Q_V^2} = \frac{u^2(\Delta M)}{\Delta M^2} + \frac{u^2(t)}{t^2} + \frac{u^2(M_{mol})}{M_{mol}^2} + \frac{u^2(R)}{R^2} + \frac{u^2(T_{ref})}{T_{ref}^2} + \frac{u^2(p_{ref})}{p_{ref}^2} \quad (5)$$

The last five terms in this equation can be obtained directly as will be shown in Sec. 4.2; though, a more detailed analysis is required for the first term. In order to perform such analysis, consider again Eq. 1 in its second form. The following sensitivity coefficients can be computed:

$$\frac{\partial \Delta M}{\partial \rho_2} = \Delta V + V_1;\ \frac{\partial \Delta M}{\partial \rho_1} = -V_1;\ \frac{\partial \Delta M}{\partial \Delta V} = \rho_2\ ;\ \ \frac{\partial \Delta M}{\partial V_1} = \rho_2 - \rho_1$$

Since in Eq. 1 the quantities ρ_1 and ρ_2 are correlated, it is also necessary to consider the covariance term:

$$Cov(\rho_1, \rho_2) = \rho_0^2 \cdot \left[\frac{u^2(p_0)}{p_0^2} + \frac{u^2(T_0)}{T_0^2}\right] \quad (6)$$

Where the subscript 0 indicates the average between the corresponding initial and final quantities, under the hypothesis that variations of the thermodynamic conditions are small.

Eq. (6) was obtained by replacing the density with its expression as a function of p and T, and developing the relevant equations for covariance, by considering small variations between initial and final conditions. The sensitivity coefficient for the covariance term is:

$$\frac{\partial \Delta M}{\partial \rho_1} \cdot \frac{\partial \Delta M}{\partial \rho_2} = -V_1 \cdot (\Delta V + V_1) \quad (7)$$

It is then possible to express the absolute standard uncertainty associated to the variation of mass within the prover as follows:

$$u^2(\Delta M) = (\Delta V + V_1)^2 \cdot u^2(\rho_2) + (\rho_2)^2 \cdot u^2(\Delta V) + (\rho_2 - \rho_1)^2 \cdot u^2(V_1) + (V_1)^2 \cdot u^2(\rho_1) - 2 \cdot V_1 \cdot (\Delta V + V_1) \cdot \rho_0^2 \cdot \left[\frac{u^2(p_0)}{p_0^2} + \frac{u^2(T_0)}{T_0^2}\right] \quad (8)$$

Uncertainties associated to the densities are expressed according to their dependency on the thermodynamic conditions. After developments and simplifications, one obtains:

$$u^2(\Delta M) = \Delta V^2 \cdot \rho_0^2 \cdot \left[\frac{u^2(p_0)}{p_0^2} + \frac{u^2(T_0)}{T_0^2}\right] + \rho_0^2 \cdot u^2(\Delta V) + (\rho_2 - \rho_1)^2 \cdot u^2(V_1) \quad (9)$$

and, in relative form:

$$\frac{u^2(\Delta M)}{\Delta M^2} = \left[\frac{u^2(p_0)}{p_0^2} + \frac{u^2(T_0)}{T_0^2}\right] + \frac{u^2(\Delta V)}{\Delta V^2} + \frac{(\rho_2 - \rho_1)^2}{\rho_0^2} \cdot \frac{V_1^2}{\Delta V^2} \cdot \frac{u^2(V_1)}{V_1^2} \quad (10)$$

which can be replaced in equation (5) to give:

$$\frac{u^2(Q_V)}{Q_V^2} = \left[\frac{u^2(p_0)}{p_0^2} + \frac{u^2(T_0)}{T_0^2}\right] + \frac{u^2(\Delta V)}{\Delta V^2} + \frac{(\rho_2-\rho_1)^2}{\rho_0^2} \cdot \frac{V_1^2}{\Delta V^2} \cdot \frac{u^2(V_1)}{V_1^2} + \frac{u^2(t)}{t^2} + \frac{u^2(M_{mol})}{M_{mol}^2} + \frac{u^2(R)}{R^2} + \frac{u^2(T_{ref})}{T_{ref}^2} + \frac{u^2(p_{ref})}{p_{ref}^2}$$

(11)

Since the present paper focuses on the geometrical calibration of the piston, the uncertainty sources associated to this calibration (diameter and displacement) are discussed separately in Sec. 4.1, while sources associated to the measurement system, to the measurement technique and to the environment (instruments, ambient conditions, etc.) are discussed in Sec. 4.3.

4.1 Geometrical calibration of MeGas

The geometrical calibration of MeGas consists in the evaluation of the mean diameter of the piston and of the piston displacement (by calibrating the MeGas encoder on site) in order to make the piston diameter and displacement traceable to the primary standard of length.

The piston diameter has been evaluated by means of two linear encoders along seven generatrices of the cylindrical piston (see Fig. 3 and Fig. 4). The piston displacement has been evaluated by calibration of the encoder with an interferometer; the interferometer was placed below the MeGas base, the laser ray passing through the bore in the base providing the facility in- and outflow (see Fig. 5 and Fig. 6).

The diameter and the displacement measurement chains are acquired simultaneously according the following sequence:

1. the linear encoders are positioned on the chosen generatrix and zeroed on the reference bar;
2. the temperature inside the chamber, the pressure and humidity in the laboratory are recorded;
3. outputs from the interferometer and the linear encoders are recorded during several vertical translations (up- and downwards) of the piston; each translation is 1.28 m long with a 1 mm step, providing thus 1280 diameter measurements on each run;
4. the temperature inside the chamber, the pressure and humidity in the laboratory are recorded again;
5. after (at least) 7 repetitions the linear encoders are zeroed again; steps (1) to (4) are then repeated for another generatrix.

The piston diameter could thus be estimated as the average of 93 x 1280 diameter acquisitions.

Great care has been taken to allow the structure to settle after the operator disturbed its temperature, by monitoring the reference bar temperature and that of the air inside the cylinder.

Full details of the procedure and complete measurement results are reported in [8] and [10]. Operations necessary to prepare the MeGas facility are detailed in [9].

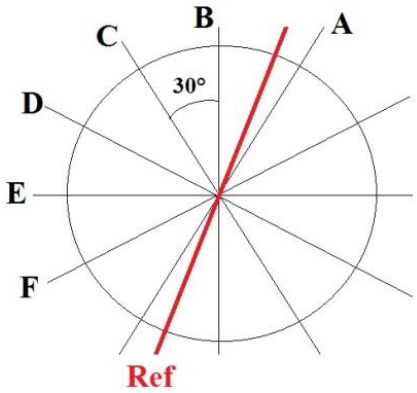

Fig. 3. Top view sketch of the piston with the positions of generatrices;

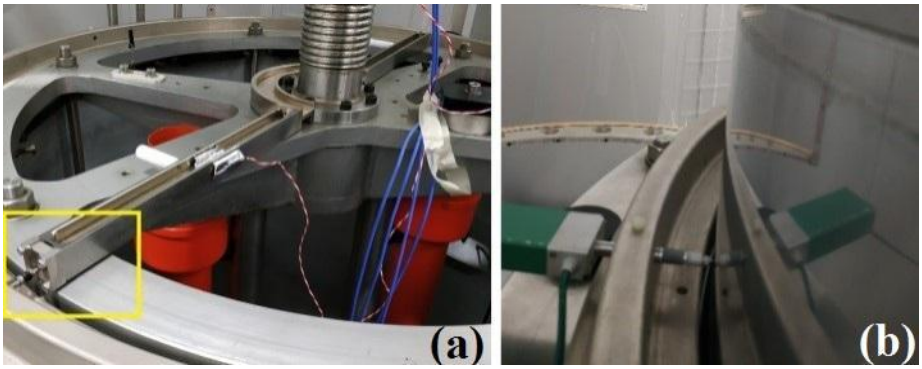

Fig. 4. (a) – Linear encoder zeroed on the reference bar (yellow frame); (b) - linear encoder during measure along one generatrix of the cylindrical piston.

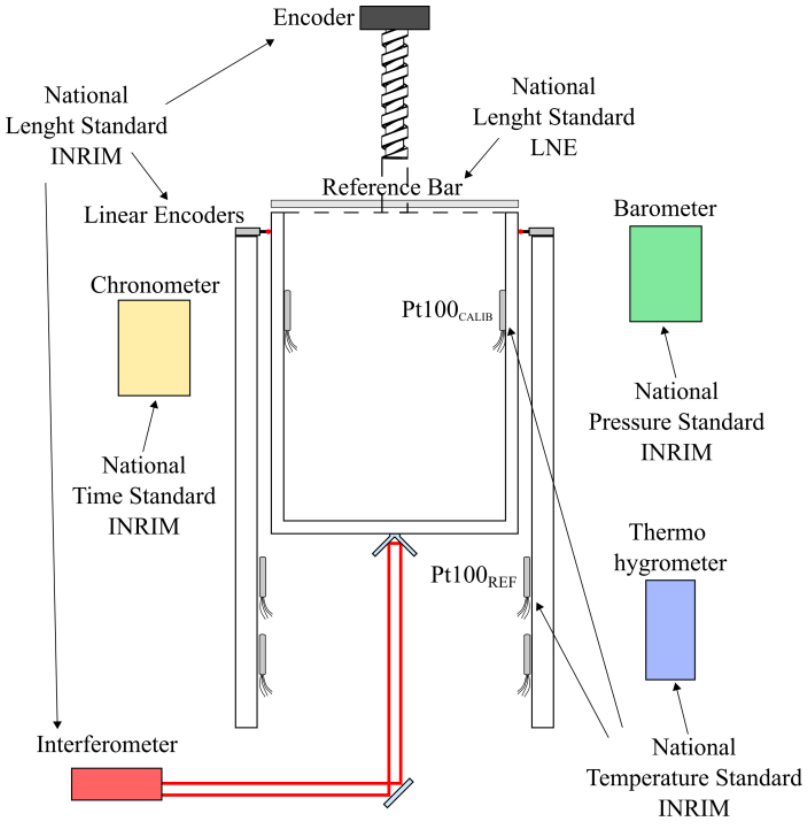

Fig. 5. Scheme of the measurement chain for MeGas, geometrical calibration

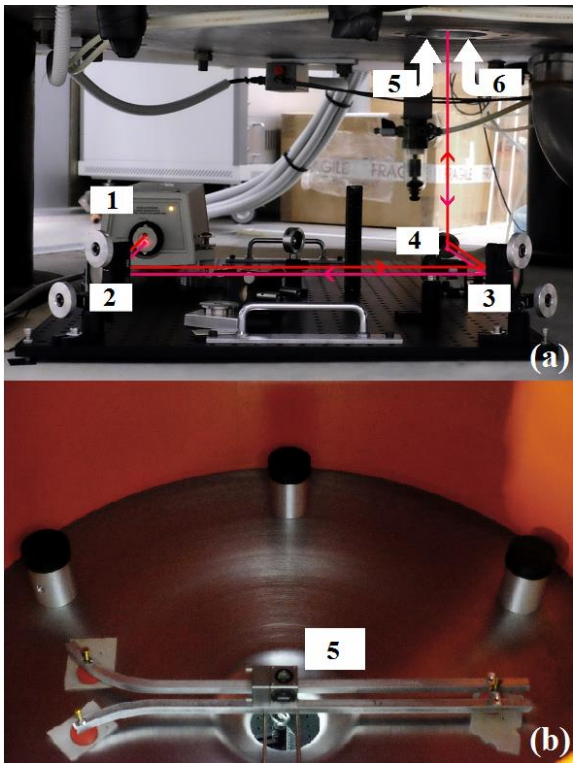

Fig. 6. (a) - Red arrows indicate the laser path. 1: interferometer, 2, 3 and 4: folding mirrors; 5: beam splitter + corner cube (visible in Fig. 6 (b)); 6: corner cube positioned on the piston inferior surface (not visible in figure); the total dead path length is of about 200 mm. (b) – 5: beam splitter + corner cube (realizing the reference arm) placed on the internal surface of the base of the chamber

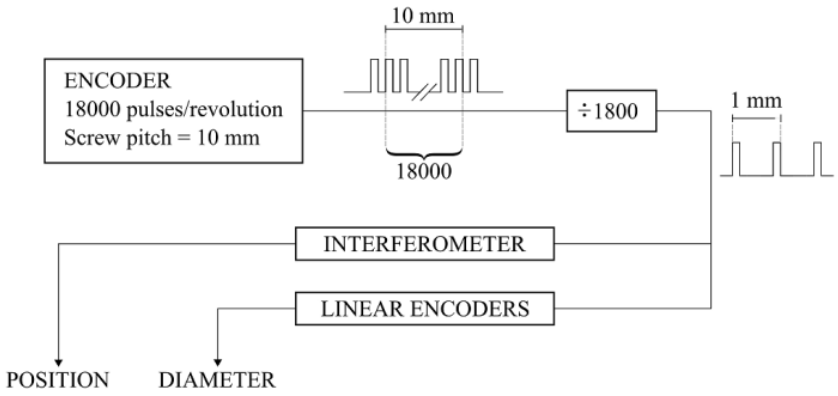

Fig. 7. Acquisition trigger block scheme.

4.1.1 Piston diameter

According to the measurement procedure applied, the diameter of a singular acquisition is evaluated as:

$$d_{i,j} = \left(\Delta L_{i,j} - \Delta L_{REF,j}\right) + L_{REF} \quad (12)$$

with i=1…1280 and j=1…93, where $\Delta L_{i,j}$ is the i-th acquisition of the j-th measure and $\Delta L_{REF,j}$ is the corresponding reference output obtained as the mean value of the measurements results ($\Delta L_{REF,1,j}$ and $\Delta L_{REF,2,j}$) obtained at different times (see point 1 and point 5 in the action list of Sec. 4.1) . The value of the reference bar is given by means of the reference bar calibration certificate The corresponding value in the most recent certificate by LNE is:

$$L_{REF} = (0.999252 \pm 0.000005) \text{ m} \quad (13)$$

The mean diameter over the 1280 acquisitions for the j-th measure is:

$$\underline{d_j} = \underline{\Delta L_j} - \Delta L_{REF,j} + L_{REF} \quad (14)$$

Finally, the mean diameter of the piston over the 93 measures is computed as:

$$\underline{d} = \frac{1}{93} \cdot \sum_{j=1}^{93} \underline{d_j} \quad (15)$$

The uncertainty associated to the single acquisition of the diameter, corresponding to the uncertainty of the measurement chain (Type B uncertainty), can be computed as:

$$u\left(d_{i,j}\right) = \sqrt{u_{CERT}^2(\Delta L) + u_{RES}^2(\Delta L) + u^2\left(\Delta L_{REF,j}\right) + u^2(L_{REF})} \quad (16)$$

where the value $u_{CERT}(\Delta L)$ is derived from the calibration certificate of the linear encoders, the value $u_{RES}(\Delta L)$ is associated to the linear encoders resolution, the value $u(\Delta L_{REF,j})$ is associated to the encoder zeroing on the reference bar and finally the standard uncertainty $u(L_{REF})$ is derived from the reference bar calibration certificate.

Each linear encoder was calibrated in INRIM. The uncertainty associated with each linear encoder was assessed by assuming a rectangular distribution with a semi-amplitude equal to the maximum correction of the reading which has to be applied according to the certificate. The uncertainty associated with the certificate $u_{CERT}(\Delta L)$ is the sum of the uncertainties associated to each encoder and the uncertainty associated with corrections, giving:

$u_{CERT}(\Delta L) = 2.19 \cdot 10^{-6}$ m.

The uncertainty associated to linear encoder resolution has been estimated to be $u_{RIS}(\Delta L) \approx 3 \cdot 10^{-8}$.

The uncertainty associate to the zeroing of the linear encoder system on the reference bar is computed assuming a rectangular distribution over the two measured values for each j-th measure:

$$u(\Delta L_{REF,j}) = \sqrt{\frac{(\Delta L_{REF,1,j} - \Delta L_{REF,2,j})^2}{12}} \quad (17)$$

and its numerical value is found to be 1.5 μm approximately. With the value of $u(L_{REF}) = 5\ \mu m$ as reported on the calibration certificate of the reference bar, the uncertainty associated to the mean diameter of the j-th measure is evaluated as:

$$u(\underline{d_j}) = \sqrt{\sigma^2(\underline{d_j}) + u^2(d_{i,j})} \quad (18)$$

where $u(d_{i,j}) = 5.7 \cdot 10^{-6}\ \boldsymbol{m}$ according to Eq. 16 and the value of $\sigma\ (\underline{d_j})$ varies from $2.0 \cdot 10^{-6}\ \boldsymbol{m}$ to $3.4 \cdot 10^{-6}\ \boldsymbol{m}$ among all the 93 measurement distributions.

The standard deviation of mean diameter calculated from the 7 generatrices (see Table 2) is $\sigma\ (\underline{d}) = 2 \cdot 10^{-5}\ m$

The mean diameter uncertainty is calculated, similarly to Eq. 18, as:

$$u(\underline{d}) = \sqrt{\sigma^2\ (\underline{d}) + u^2(d_{i,j})}\ =\ 2.1 \cdot 10^{-5}\ m \quad (19)$$

The mean diameter in the working range was therefore evaluated to be equal to:

$$\underline{d} = 0.99950\ \pm\ 4.2 \cdot 10^{-5}\ \boldsymbol{m} \quad (20)$$

In Fig. 8 and Fig. 9 the mean diameter for each generatrix and the overall mean diameter are shown.

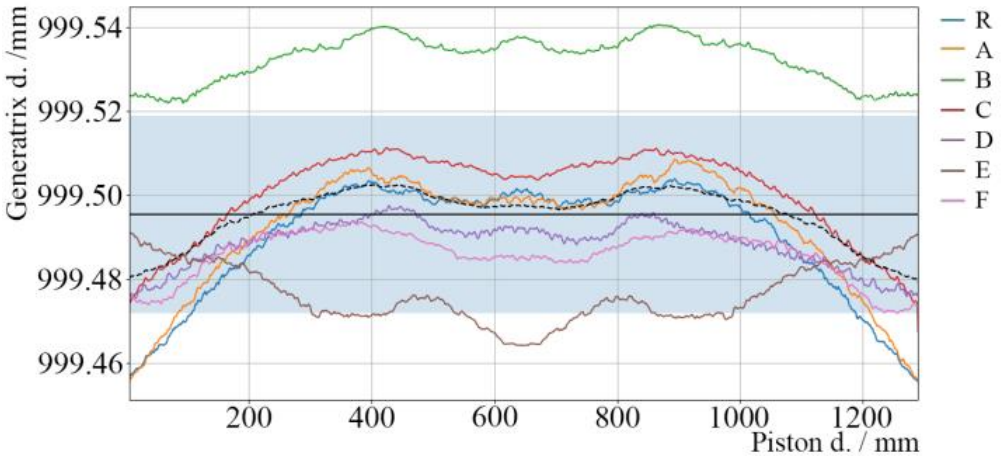

Fig. 8. Piston full travel: mean diameter for each generatrix (in color) and mean of the means (dashed black) as a function of piston displacement for the piston full travel. The continuous black line represents the mean over the piston full travel, with its standard deviation indicated by the colored area.

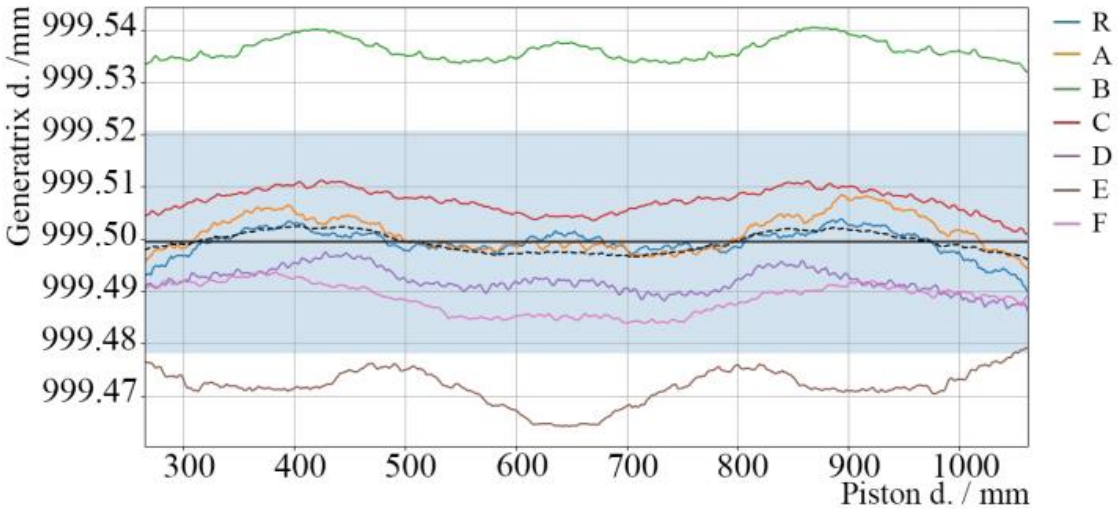

Fig. 9. Piston working range: mean diameter for each generatrix (in color) and mean of the means (dashed black) as a function of piston displacement for the piston displacement limited to the working range The continuous black line represents the mean over the piston, with its standard deviation indicated by the colored area.

The mean diameter for each generatrix is tabulated below; the mean diameter and its standard deviation are also shown.

generatrix	$\underline{d_j}$ **/ m**
R	**0.999496**
A	**0.999498**
B	**0.999533**
C	**0.999504**
D	**0.999489**
E	**0.999469**
F	**0.999486**
$\underline{\boldsymbol{d}}$ **= 0.99950 m and** $\sigma\left(\underline{\boldsymbol{d}}\right) = 2 \cdot 10^{-5}$ **m**	

Table 2. Mean diameter $\underline{d_j}$ for each generatrix and mean diameter of the piston $\underline{\boldsymbol{d}}$

4.1.2 Piston displacement

In an interferometric measure, the displacement L of an object is obtained by multiplying the number of fringes N by half the wavelength λ of the laser used.

$$L = N \cdot \frac{\lambda}{2} \tag{21}$$

In order to obtain the actual displacement L of the piston a correction factor for the vacuum wavelength and for the refractive index has to be applied to the interferometer output L_{interf}. The actual displacement L is therefore computed as:

$$L = L_{interf} \cdot \frac{\lambda_0}{\lambda_{0,interf}} \cdot \frac{n_{interf}}{n} \tag{22}$$

where λ_0 is the laser vacuum wavelength obtained from the calibration certificate, $\lambda_{0,interf}$ and n_{interf} are the vacuum wavelength and the refractive index used by the interferometer electronics for the computation of L_{interf}, which is a function of $\lambda_{0,interf}$ and n_{interf}; the refractive index n is calculated using the Edlén formula as given in Appendix A-IV of the Engineering Metrology Toolbox of NIST, Eq. A49 [12] and recalled in Eq. 23 for clearness, where T, p and RH are, respectively, the values of temperature, pressure and relative humidity during the measurement, obtained as the respective means of the initial ($T_{in,j}$, $p_{in,j}$, $RH_{in,j}$) and the final conditions ($T_{fin,j}$, $p_{fin,j}$, $RH_{fin,j}$) for every travel j=1…93 of the piston.

$$n(\lambda_0, T, p, RH) = n_{tp}(\lambda_0, T, p) - 10^{-10} \cdot p_V(RH, T) \cdot 292.75 \cdot \frac{3.7345 - 0.0401 \cdot S(\lambda_0)}{T + 273.15} \tag{23}$$

Authors decided to not add further details in this work about the computation of the refractive index n because it is a too much specific dimensional metrology topic. However, all details on the computation of n can be found in [11], [12] and [13].

According the Eq. 22, the displacement $L_{i,j}$ for a single acquisition can be calculated as:

$$L_{i,j} = L_{i,j,interf} \cdot \frac{\lambda_0}{\lambda_{0,interf}} \cdot \frac{n_{interf}}{n_{i,j}} \tag{24}$$

with *i*=1…1280 and *j*=1…93. Actually, the difference $\delta L_j = L_{i+1,j} - L_{i,j}$between two consecutive displacements is more useful for MeGas calibration purposes. As for the diameter evaluation, it has been considered the average difference for the j-th measure:

$$\underline{\delta L_j} = \frac{1}{1279} \cdot \sum_{i=1}^{1279} \quad (L_{i+1,j} - L_{i,j})$$

(25)

The average difference over the 93 measurements is computed:

$$\underline{\delta L} = \frac{1}{93} \cdot \sum_{j=1}^{93} \quad \underline{\delta L_j} \tag{26}$$

The uncertainty associated to the $\underline{\delta L}$ has been obtained as the sum of squares of its type A and type B uncertainty contributions:

$$u(\underline{\delta L}) = \sqrt{{u_A}^2(\underline{\delta L}) + {u_B}^2(\underline{\delta L})} \tag{27}$$

where:

$$u_A(\underline{\delta L}) = \sigma_{MAX}(\underline{\delta L_j}) \tag{28}$$

and

$$u_B(\underline{\delta L}) = u_B(\underline{\delta L_j})|_{j=1\ldots93} = \delta L_{interf} \cdot \frac{\lambda_0}{\lambda_{0,interf}} \cdot \frac{n_{interf}}{n} \cdot \sqrt{\frac{u^2(\delta L_{interf})}{{\delta L_{interf}}^2} + \frac{u^2(\lambda_0)}{{\lambda_0}^2} + \frac{u^2(n)}{n^2}} \tag{29}$$

The quantities $\lambda_{0,interf}$ and n_{interf}, used by the electronics of the interferometer, are considered two constants and therefore without uncertainty. The uncertainty associated to the displacement measure δL_{interf}, has been calculated with the usual propagation formula:

$$u(\delta L_{interf}) = \sqrt{u^2(\delta L_{interf,cos}) + u^2(\delta L_{interf,Abbe}) + u^2(\delta L_{interf,dp})}$$

(30)

where $u(\delta L_{interf,cos})$ is the uncertainty associated to the cosine error, $u(\delta L_{interf,Abbe})$ is the uncertainty associated to the Abbe error and $u(\delta L_{interf,dp})$ is the uncertainty associated with the dead path. The contribution due to the interferometer resolution has been considered negligible.

The errors (cosine, Abbe and dead path) were assumed equal to zero and their contributions were taken into account by including them into the uncertainty computation.

The uncertainty associated with the cosine error has been evaluated from a rectangular PDF whose amplitude is the estimation of the maximum allowed misalignment of the laser beam, obtained by applying a safety factor greater than 10 to the maximum misalignment of the laser beam estimated by using an electronic position sensor.

The uncertainty associated with the Abbe error has been evaluated from the quality of the piston manufacturing (motion-measurement axes translation) and the maximum "reasonable" rotation and assuming, again, a rectangular PDF.

The uncertainty associated with the dead path error has been evaluated from an estimate of the maximum refractive index variation in the dead path, and assuming a rectangular PDF of equal amplitude.

Further details of the three contributions in Eq. 30 can be found in [8] and [11].

The results of this analysis are summarized in Table 3.

The second uncertainty contribution in Eq. 29, namely $u(\lambda_0)$, is derived from the calibration certificate of the interferometer and is equal to $u(\lambda_0) = 1.5 \cdot 10^{-15}$ m.

Finally the uncertainty associated with the refractive index u(n) has been evaluated from the Edlen empirical formula (Eq. 23) used for the computation of the refractive index n. In particular, the uncertainty associated to the refractive index n is calculated with the following propagation formula:

$$u(n) = \sqrt{\left(\frac{\partial n}{\partial \lambda_0}\right)^2 \cdot u^2(\lambda_0) + \left(\frac{\partial n}{\partial t}\right)^2 \cdot u^2(T) + \left(\frac{\partial n}{\partial p}\right)^2 \cdot u^2(p) + \left(\frac{\partial n}{\partial RH}\right)^2 \cdot u^2(RH)} \quad (31)$$

The first term $u(\lambda_0)$ has already been described, the second, third and fourths terms are due to the ambient parameters (T, p and RH) variation during the measurement.

The evaluation of the uncertainty of these three terms is not reported here. An example of values obtained by the ambient parameters uncertainty analysis follows in Table 4 and are obtained taking into account: the resolution of the instruments, their accuracy, the calibration certificate of the instruments and the standard deviation of the acquired samples. The example in Table 4 reports the computation of the reflective index uncertainty u(n) by means of the maximum standard uncertainty evaluated for every environmental parameter during all the measurements periods. During the 15-day measurement session, the average uncertainties in the refractive index were $u(n)_{average} = 3.68 \cdot 10^{-8}$

with a peak-peak variation of $u(n)_{max} = 4.76 \cdot 10^{-8}$. The value $u(n)_{average}$ is used for the final computation of uncertainty associated to the piston displacement.

Finally, the uncertainty associated to the piston displacement $\underline{\delta L}$ can be computed according to Eq. 27 as follow:

$$u(\underline{\delta L}) = \sqrt{{\sigma_{MAX}}^2(\underline{\delta L_j}) + \left(\delta L_{interf} \cdot \frac{\lambda_0}{\lambda_{0,interf}} \cdot \frac{n_{interf}}{n}\right)^2 \cdot \left(\frac{u^2(\delta L_{interf})}{{\delta L_{interf}}^2} + \frac{u^2(\lambda_0)}{{\lambda_0}^2} + \frac{u^2(n)}{n^2}\right)} \quad (32)$$

$u(\underline{\delta L}) = 1.4 \cdot 10^{-6}$ m.

Table 5 summarizes the value of contributions expressed in Eq. 32.

For the MeGas functioning it is necessary to estimate the displacement of the piston by means of the facility encoder and not by means of the interferometer that is used only during the procedure of the geometrical calibration of the piston. To do this the transfer function of the encoder (ERA180 Heidenain, with a resolution of 18000 pulse per round) is applied to the encoder output itself:

$$\delta L_{trans\_funct.} = \left(\frac{1}{1800} \cdot N_{enc}\right) \cdot 1 \cdot 10^{-3}\text{m} \quad (33)$$

where N_{enc} is the number of pulses output of the MeGas encoder for a displacement δL of the piston. Finally, according to the reported analysis, the mean displacement of the piston evaluated taking into account the encoder transfer function was found to be:

$$\underline{\delta L} = \left(\frac{1}{1800} \cdot N_{enc}\right) \pm 2.8 \cdot 10^{-6}\text{ m} \quad (34)$$

Fig. 10 shows a detail of the step size variation caused by the screw pitch.

Standard uncertainty	**Probability Density Function**
$u(\delta L_{interf,cos})$= 3·10-8 m	rectangular
$u(\delta L_{interf,Abbe})$= 5.8·10-7 m	rectangular
$u(\delta L_{interf,dp})$= 1.2·10-8 m	rectangular
$u(\delta L_{interf})$= 5.8·10-7 m	

Table 3. Contributions of uncertainty associated to the measured displacement δL_{interf}.

Standard Uncertainty	**Probability Density Function**
$u(\lambda_0)$= 1.5·10^{-15} m	normal
$u(T)_{max}$= 0.02 K; $u(t)_{max}$ = 0.02 °C	normal
$u(p)_{max}$= 4.30 Pa	normal
$u(RH)_{max}$=1.75%	normal
Sensibility Coefficient (typical value)	
$\frac{\partial n}{\partial \lambda_0}$=-1.2·10^{-8} nm^{-1}	$\frac{\partial n}{\partial p}$=2.5·10^{-9} Pa^{-1}
$\frac{\partial n}{\partial t}$=-1·10^{-6} K^{-1}	$\frac{\partial n}{\partial RH}$=-2·10^{-8}
$u(n)$ = **2.27·10^{-8}**	

Table 4. Example of computation of uncertainty associated to the refractive index $u(n)$.

Standard uncertainty	**Probability density function**
$\sigma_{MAX}(\underline{\delta L_j})$= 1.2·10^{-6} m	normal
$u(\delta L_{interf})$= 5.8·10^{-7} m	rectangular
$u(\lambda_0)$= 1.5·10^{-15} m	normal
$u(n) = u(n)_{average}$= 3.68·10^{-8}	rectangular
$u(\underline{\delta L}) = 1.4\ \mu m$	

Table 5. Contributions of uncertainty associated to the piston displacement.

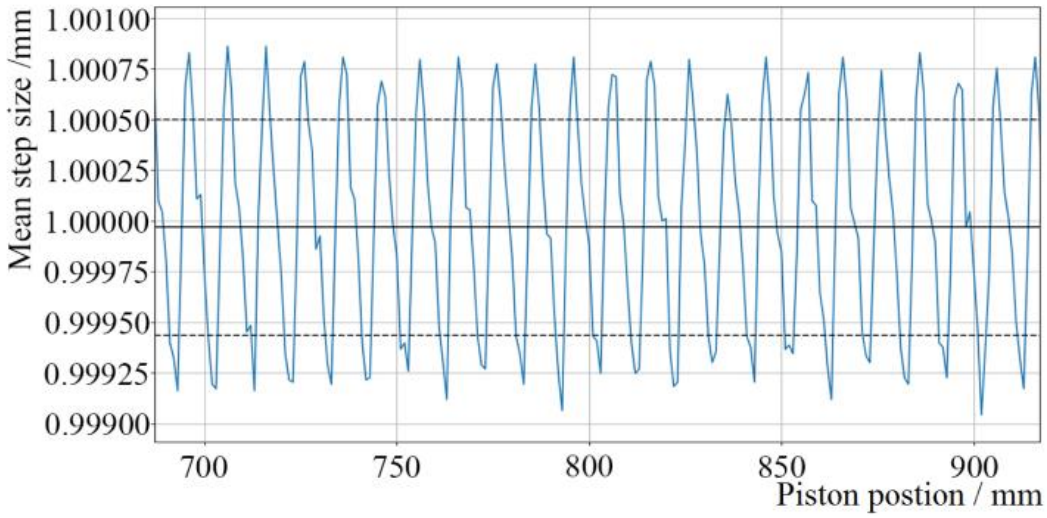

Fig. 10. Mean step size as a function of piston displacement over a portion of its travel. The continuous black line is the mean step over the piston travel range, the dashed lines indicates its standard deviation, showing the step size variation caused by the screw pitch.

As a comparison, the calibration performed in 1999 provided a mean diameter of 999.51 mm with an associated uncertainty of 0.02 mm, and the uncertainty associated to the displacement reading performed by the encoder was found to be 1,5 μm

4.2 Displaced Volume Uncertainty

As described in Sec. 2.2.1, the (nominal) volume of gas displaced by the piston can be computed from the piston displacement and its section (obtained from the diameter):

$$\Delta V = \underline{\delta L} \cdot \pi \left(\frac{\underline{d}}{2}\right)^2 \tag{35}$$

Eq. 35 is a simple multiplicative model, therefore its uncertainty can be easily obtained applying the usual formulations for this type of models [10]:

$$\frac{u(\Delta V)}{\Delta V} = \sqrt{\left(\frac{u(\underline{\delta L})}{\underline{\delta L}}\right)^2 + 2 \cdot \left(\frac{u(\underline{d})}{\underline{d}}\right)^2} \tag{36}$$

Furthermore, an uncertainty term associated to possible in-use thermal deformations of the driving screw $\left(\frac{u(\Delta V)}{\Delta V}\right)_{T,S}$ was evaluated. Considering the maximum temperature variations described earlier, this term was evaluated to a relative value of 0.00036% (*i.e.* $\left(\frac{u(\Delta V)}{\Delta V}\right)_{T,S} = 0.0000036$), which will be added in quadrature to equation (36) to give:

$$\frac{u(\Delta V)}{\Delta V} = \sqrt{\left(\frac{u(\underline{\delta L})}{\underline{\delta L}}\right)^2 + 2 \cdot \left(\frac{u(\underline{d})}{\underline{d}}\right)^2 + \left[\left(\frac{u(\Delta V)}{\Delta V}\right)_{T,S}\right]^2} \quad (37)$$

Substituting the values obtained in Sec. 4.1.1. and Sec. 4.1.2, one will obtain that the uncertainty on the displaced volume is composed by two essentially constant terms, and by a term whose value is reduced as the piston displacement increases. It will be therefore possible to limit the overall uncertainty by increasing the piston displacement, which is the reason why MeGas procedures prescribe a minimum volume (*i.e.* a minimum displacement) for calibrations.

Table 6 reports an example of evaluation of the uncertainty associated with the displaced volume u(ΔV) in the case of ΔV=50 L and ΔV=100 L. It can be observed in Table 6 that the displaced volume relative uncertainty u(ΔV)/ ΔV is a decreasing function of the displacement alone under the assumptions discussed in the present paper. Additionally, it can be seen that, for such values of the displacement, the uncertainty components associated to the piston diameter and displacement are of the same order of magnitude.

ΔV=50 L	
Standard uncertainty	**Probability density function**
$\frac{u(\underline{\delta L})}{\underline{\delta L}} = 2.197 \cdot 10^{-5}$	Rectangular
$\frac{u(\underline{d})}{\underline{d}} = 2.1 \cdot 10^{-5}$	Normal
$\left(\frac{u(\Delta V)}{\Delta V}\right)_{T,S} = 3.6 \cdot 10^{-6}$	Rectangular
$\frac{u(\Delta V)}{\Delta V} = 3.71 \cdot 10^{-5} \quad \rightarrow \quad u(\Delta V) = 1.86 \cdot 10^{-3} L$	
ΔV=100 L	
Standard uncertainty	**Probability density function**
$\frac{u(\underline{\delta L})}{\underline{\delta L}} = 1.098 \cdot 10^{-5}$	Rectangular
$\frac{u(\underline{d})}{\underline{d}} = 2.1 \cdot 10^{-5}$	Normal
$\left(\frac{u(\Delta V)}{\Delta V}\right)_{T,S} = 3.6 \cdot 10^{-6}$	Rectangular
$\frac{u(\Delta V)}{\Delta V} = 3.19 \cdot 10^{-5} \quad \rightarrow \quad u(\Delta V) = 3.19 \cdot 10^{-3} L$	

Table 6. Example of uncertainties computation for a nominal displaced volume of 50 L (corresponding to a piston displacement of about 63.7 mm) compared to a nominal displacement volume of 100 L (corresponding to a piston displacement of approximately 127 mm)

4.3 Other Uncertainty Sources

Considering again Eq. 11, it can be observed that several components influence the final result in addition to the uncertainty associated with the measured volume. The following subsections are dedicated to the analysis of such components.

4.3.1 Pressure measurement

Pressures are measured using a barometer traceable to the Italian National Pressure Standard; the standard uncertainty associated to the barometer is obtained by considering the calibration uncertainty, taken directly from the relevant calibration certificate, the standard deviation of the calibration coefficient at the various calibration pressures, and the drift uncertainty, which is estimated based on the historical series of calibrations. Since the two pressure measurements are strongly correlated because they are performed through the same instrument, the uncertainty associated with their average can be considered equal to the average of their uncertainties, *i.e.* essentially the uncertainty associated with each measurement. As an example, data from the certificate presently used provide an overall standard uncertainty of 2.82 Pa, approximated to 3 Pa; the pressure within the prover can be considered constant since the piston movement is sufficiently slow to rule out any dynamic pressure variations. Since the operating pressure of the piston is essentially the ambient pressure, which at the elevation of the laboratory is on average of about 98 kPa, it can be stated that $\frac{u(p_0)}{p_0} = \frac{3}{98000} = 3.1 \cdot 10^{-5}$

4.3.2 Temperature measurement

Temperature within the chamber is measured using a set of 8 PT100 probes traceable to the Italian National Temperature Standard, positioned within the chamber; in particular, one of the probes stands 5 cm over the bore for gas exit, while the other 7 are placed within the gap between the piston and the chamber along three circumferences at different heights spanning most of the chamber height. By considering the calibration uncertainty and the estimated drift uncertainty, the total uncertainty associated to a single probe (PT100) is 0.01 K. The size of the chamber is quite large, therefore spatial variations of temperature are possible, albeit they will be mitigated by the mixing induced by the piston movements and by the fact that the temperature in the room is controlled as described earlier; the measurements performed with the 8 probes allow to determine an average temperature within the chamber, whose uncertainty can be evaluated as the standard deviation of the values measured by the different probes, and is computed

at every temperature measurement (initial and final); a typical value for this contribution is of 0.02 K; this low value is justified by the mitigating effects described earlier. The composition in quadrature of the probes' uncertainties and of the averaging uncertainty leads to a (typical) value of 0.0223 K, approximated to 0.025 K, and therefore, considering a typical working temperature of 20 °C (293.15 K), it comes out that

$$\frac{u(T\ )}{T} = \frac{0.025}{293.15} = 8.5 \cdot 10^{-5}$$

4.3.3 Initial volume estimate

The initial volume of the measurement is evaluated by adding the dead volume estimate to the currently measured displaced volume. The dead volume is estimated through geometrical computations based on the design dimensions of the piston and the cylinder; the relative standard uncertainty associated with this value is estimated to be of about 3% of the dead volume. Since the relative uncertainty associated with the measurement of the displaced volume is far smaller than this value, it can be considered that the relative uncertainty of the initial volume corresponds to the relative uncertainty associated with the dead volume. Notice that applying the estimate for the relative uncertainty of the dead volume to the whole initial volume provides an estimate which is more and more detrimental as the piston rises within the prover. Though, due to the very small sensitivity coefficient associated with the initial volume (see Sec. 4 for details and Table 7 for an example), this does not substantially impact the final uncertainty estimate of the whole test rig.

4.3.4 Time measurement

Time is measured through a quartz chronometer included in the control system of the test rig; this chronometer is periodically checked against a precision chronometer traceable to the Italian National Time Standard. The uncertainty associated to the quartz chronometer due to this checking procedure is estimated precautionary to 1 ms; dividing this value by the minimum test time of 60 s, one gets for the maximum value of the time uncertainty:

$$\frac{u(t)}{t} = \frac{0.001}{60} = 1.7 \cdot 10^{-5}$$

4.3.5 Gas Properties Estimate

The gas properties M_{mol} and R are obtained from suitable databases; in particular, as of the present date, the molar mass, together with its uncertainty, is obtained from the IUPAC Technical Report [14]; as an example, when pure molecular nitrogen (N_2) is used, such tables provide $M_{mol} = 28.013710 \pm 0.00085$, *i.e.* a relative uncertainty of 0.003%. The gas composition is not considered as a possible source of uncertainty in the case of pure gases (which is the case considered for the definition of the CMC) since the laboratory uses gas with purity of at least 5.5 (99.9995% pure). Regarding the molar gas constant R, this value is taken from the CODATA recommended values list maintained by NIST [9]; since the 2018 revision, this value is considered as exact and therefore not affected by uncertainty.

4.3.6 Reference Conditions

The reference conditions used for the normalization of the results can have two sources, depending on the application. In the simplest case, such conditions are standardized conditions, therefore they are exact values not affected by any uncertainty; in this case the last two terms in Eq. 11 are zero. Notice, though, that in this case an additional uncertainty term associated with the method used by the DUT for the normalization of its output to the same reference conditions must be evaluated, but this is outside the scope of the present paper. On the other hand, if the reference conditions are defined as the ones at the DUT, the last two terms of Eq. 11 correspond to the uncertainty associated to the measurement of such conditions, which can be measured either by instruments associated to the DUT itself, or by the instrumentation available to the laboratory. In both cases, the evaluation of these terms is performed in the same way as discussed in Sec. 4.3.1 and Sec. 4.3.2 by replacing the values indicated there with the corresponding values of the employed instrumentation and the estimate for the fluctuation of the thermodynamic conditions at the DUT.

4.3.7 Leaks

The presence of leaks from the machine openings is periodically checked by creating a pressure differential with the ambient equal to the maximum operating pressure of the piston; the pressure within the piston is then monitored for at least one hour to check for possible deviations, while checking the corresponding temperature variations and compensating for them; experimental results show that leakages from the piston are negligible.

4.3.8 Compressibility factor Z

Possible deviations of the gas behavior from the ideal gas law, which is assumed in the evaluation of the densities, were considered by computing the variations of the compressibility factor Z in the case of pure nitrogen (typically used in the test rig) through the software REFPROP Mini by NIST [15]; the results show that for a variation of 2000 Pa and 0.2 K (which are well beyond the admissible variations of conditions within the prover during one test, but might represent the difference between conditions in the test rig and at the DUT in unfavorable conditions) the variation of the compressibility factor is within 7 parts per million; since this value is largely smaller than other uncertainty components, it is considered as negligible.

5. Uncertainty budget

This section summarizes the different uncertainty contributions to define the uncertainty budget associated with the primary gas flow standard at MeGas.

The gas flow is computed according to Eq. 11 here reported for the reader.

$$\frac{u^2(Q_V)}{Q_V^2} = \left[\frac{u^2(p_0)}{p_0^2} + \frac{u^2(T_0)}{T_0^2}\right] + \frac{u^2(\Delta V)}{\Delta V^2} + \frac{(\rho_2-\rho_1)^2}{\rho_0^2}\cdot\frac{V_1^2}{\Delta V^2}\cdot\frac{u^2(V_1)}{V_1^2} + \frac{u^2(t)}{t^2} + \frac{u^2(M_{mol})}{M_{mol}^2} + \frac{u^2(R)}{R^2} + \frac{u^2(T_{ref})}{T_{ref}^2} + \frac{u^2(p_{ref})}{p_{ref}^2}$$

Table 7 shows an example of uncertainty budget in case of following typical conditions:

$p_{ref} = p_o = 98000$ Pa, $T_{ref} = T_0 = 293.15$, $\Delta V = 100$ L, $V_1 = 800$ L, flow rate = 100 L/min, measurement time = 1 min and a variation of p and T conditions of about 20 Pa and 0.1 K between the initial conditions and the final conditions of measurement corresponding for this example to: $p_1 = 97990$ Pa, $p_2 = 98010$ Pa, $T_1 = 293.10$ K, $T_2 = 293.20$ k, $\rho_0 = 1.126135$ kg/m^3 $\rho_1 = 1.12621$ kg/m^3, $\rho_2 = 1.12606$ kg/m^3.

Relative uncertainty	Probability density function	Sensitivity coefficient	Contribution	Relative weight (%)
$\frac{u(p_0)}{p_0} = \frac{3}{98000} = 3.1 \cdot 10^{-5}$	Normal	1	$9.61 \cdot 10^{-10}$	4.9
$\frac{u(T_0)}{T_0} = \frac{0.025}{293.15} = 8.5 \cdot 10^{-5}$	Normal	1	$7.225 \cdot 10^{-9}$	37.0
$\frac{u(\Delta V)}{\Delta V} = 3.19 \cdot 10^{-5}$	Normal	1	$9.61 \cdot 10^{-10}$	4.9
$\frac{u(V_1)}{V_1} = 3.0 \cdot 10^{-2}$	Rectangular	$1.1355 \cdot 10^{-6}$	$1.022 \cdot 10^{-9}$	5.2
$\frac{u(t)}{t} = \frac{0.001}{60} = 1.7 \cdot 10^{-5}$	Rectangular	1	$2.89 \cdot 10^{-10}$	1.5
$\frac{u(M_{mol})}{M_{mol}} = 3.0 \cdot 10^{-5}$	Normal	1	$9.00 \cdot 10^{-10}$	4.6
$\frac{u(R)}{R} = 0 \ (exact\ value)$	---	-	-	-
$\frac{u(T_{ref})}{T_{ref}} = \frac{u(T_0)}{T_0} = 8.5 \cdot 10^{-5}$	Normal	1	$7.225 \cdot 10^{-9}$	37.0
$\frac{u(p_{ref})}{p_{ref}} = \frac{u(p_0)}{p_0} = 3.1 \cdot 10^{-5}$	Normal	1	$9.61 \cdot 10^{-10}$	4.9
$\frac{u(Q_V)}{Q_V} = 1.40 \cdot 10^{-4}$				

Table 7. Example of computation of the relative uncertainty of the gas flow at the MeGas primary standard.

It can be observed that the main contributions to the overall uncertainty are the ones associated with the temperature measurement, as could be expected. It is also to be noticed that the other contributions, and in particular the two associated to volume measurement, have approximately the same magnitude.

Q / L/min	ΔV /L	**t / min**	$\frac{u(Q_V)}{Q_V}$ / -
100	**100**	**1**	$1.40 \cdot 10^{-4}$
50	**50**	**1**	$1.41 \cdot 10^{-4}$
10	**10**	**1**	$1.78 \cdot 10^{-4}$
1	**1**	**1**	$1.11 \cdot 10^{-3}$
1	**50**	**50**	$1.40 \cdot 10^{-4}$

Table 8. Computation of the relative uncertainty of the gas flow at the MeGas primary standard for five representative cases, at the same condition of Table 7

It can be observed that, as the delivered volume decreases, the uncertainty associated with the flow rate increases, and quite dramatically for very low volumes. This is the reason why MeGas procedures prescribe a minimum delivered volume of 50 L for measurements. It can be noticed by comparing the second and the last row that also the measurement time has an influence, but similar computations show that this effect is very small for measurement times larger than one minute, which is why MeGas procedures also prescribe a minimum measurement time of 60 s. The results discussed in the present article will be of course validated through appropriate International Comparisons; one of these comparisons is currently underway, and INRIM already performed its set of measurements, although results are not yet available.

6. Conclusions

This paper presents a complete analysis of the measurement capabilities of the MeGas gas flow standard including uncertainty. Its features, traceability chain and the uncertainty budget of the measurements it can perform have been described in detail. Special attention has been dedicated to the dimensional calibration of the piston diameter and displacement. The values obtained from this calibration are in good agreement with the one that was carried out at the piston initial installation in 1999, thus confirming the stability of the standard. This work supports the uncertainties claimed by INRIM but, above all, provides a useful guide for a study of the uncertainty associated with a general

piston proper gas flow standard. International comparisons are certainly a fundamental exercise for confirming or not the measurement capabilities of a standard, but in the event that the comparison has not been concluded successfully, the results of comparison do not provide a certain indication of what the error may be in assessing the uncertainty of the sample compared. Providing the uncertainty budget details of a primary gas flow standard can therefore be a valid tool to allow a theoretical comparison of standard as well.

References

[1] G. Cignolo, A. Rivetti, G. Martini, F. Alasia, G. Birello, G. La Piana, "The National Standard Gas Prover of the IMGC-CNR", in Proceedings of the 10th Flomeko Conference, Salvador (Brazil), 5-9 June, 2000

[2] H. Bellinga, F.J. Delhez "Experience with a high-capacity piston prover as a primary standard for high-pressure gas flow measurement", 1993, Flow Measurement and Instrumentation, 4(2): 85-89.

[3] R.F. Berg, T. Gooding, R.E. Vest "Constant pressure primary flow standard for gas flows from 0.01 cm /min to 100 cm /min (0.007–74 μmol/s)", 2014, Flow Measurement and Instrumentation, 35: 84-91.

[4] M.P. van der Beek, R. van der Brink "Gas Oil Piston Prover, primary reference values for Gas-Volume", 2015, Flow Measurement and Instrumentation, 44: 27-33.

[5] Z.P. Xu, J.Y: Dai, H.Y. Chen, D.L. Xie "Development of a reciprocating double-pistons gas prover", 2014, Flow Measurement and Instrumentation, 38: 116-120.

[6] Anonymous, 2009, Details omitted for double-anonymized reviewing

[7] Anonymous, 2010, Details omitted for double-anonymized reviewing

[8] Anonymous, 2019, Details omitted for double-anonymized reviewing

[9] Anonymous, 2019, Details omitted for double-anonymized reviewing

[10] BIPM, IEC, IFCC, ILAC, ISO, IUPAC, IUPAP, and OIML. Evaluation of measurement data — Guide to the expression of uncertainty in measurement. Joint Committee for Guides in Metrology, JCGM 100:2008.

[11] Anonymous, 2020, Details omitted for double-anonymized reviewing

[12] https://emtoolbox.nist.gov/Wavelength/Equation2.asp

[13] https://physics.nist.gov/cuu/Constants/bibliography.html

[14] Meija, Juris, Coplen, Tyler B., Berglund, Michael, Brand, Willi A., De Bièvre, Paul, Gröning, Manfred, Holden, Norman E., Irrgeher, Johanna, Loss, Robert D., Walczyk, Thomas and Prohaska, Thomas. "Atomic weights of the elements 2013 (IUPAC Technical Report)" Pure and Applied Chemistry, vol. 88, no. 3, 2016, pp. 265-291. https://doi.org/10.1515/pac-2015-0305

[15] Lemmon, E.W., Bell, I.H., Huber, M.L.and McLinden, M.O. "NIST Standard Reference Database 23: Reference Fluid Thermodynamic and Transport Properties-REFPROP, Version 10.0" , National Institute of Standards and Technology, Standard Reference Data Program, Gaithersburg, 2018.

Metrological features of the Large Piston Prover at INRIM

Abstract

INRIM realizes its flow rate standard using three distinct facilities, aimed at measuring different flow rate ranges; in particular, for the largest flow range rate (10-2600 L/min) a piston prover is used. This machine is of the volumetric type, therefore its traceability can be obtained through dimensional calibration of the piston, which has a nominal diameter of 1000 mm and a nominal stroke of 1200 mm.

The present paper describes in detail the features of the standard, its traceability chain and the uncertainty budget of the measurements it can perform. The uncertainty budget directly determines the Calibration and Measurement Capabilities claim in the range available to the test rig. A detailed analysis of the various uncertainty components will be presented and discussed. Special attention will be dedicated to the dimensional calibration of the piston, since it is of paramount importance for the determination of the main uncertainty component. This calibration is particularly challenging since, due to the large size of the piston, it must be carried on in-situ, thereby requiring a set of special adaptations with respect to a standard calibration of a cylinder. It will be shown that the calibration of the piston recently performed is in good accordance with the one that was carried out at the piston initial installation in 1999, thus confirming the stability of the standard.

Keywords

primary flow standard; volumetric calibration; uncertainty analysis; test rig development; flow calibration

1. Introduction

Accurate measurement of gas flow rate is a field whose importance is well established due to the wide range of application where such quantity is of paramount importance (*e.g.* fuel gas exchange, process gas measurement in applications connected to medical/chemical industry, etc.); presently, there is a growing need for accurate calibration of mass flow meters with various Full Scale Range (FSR), that have an increasingly wide field of application (*e.g.* for dynamical gas mixing, aerospace applications, etc.). The flow rates of interest range from fractions of cubic millimeters per second to several hundreds of liters per second. For such a range of flow rates, a robust and reliable measurement technology is the piston prover volumetric method, since it provides a carefully controlled flow of gas; its accurate measurement requires a reliable and precise knowledge of the relationship between delivered volume and

piston movement, the possibility to precisely measure the gas temperature and pressure, and the possibility of using high purity gases for the tests. INRIM operates two piston provers (in addition to a bell prover) to realize the Italian National Standard of gas flow rate. Specifically, one of the pistons is dedicated to extremely low flow rates (from ≈ 0.1 Cubic Centimeters per minute – CCM to ≈ 1.2 Liters per minute) and will not be discussed here. The piston which is the subject of the present paper is the bigger one, called MeGas, which generates flows ranging from ≈ 1 Liter per minute to ≈ 2500 Liters per minute, although the higher flow rate is usually self-limited to about 1000 Liters per minute. INRIM has operated the MeGas piston prover for several years now [1]; its features include a very accurate piston machining, reduced movement friction, accurate measurement of the piston movement and of the gas thermodynamic conditions, and temperature stabilization of the environment. Although all of these features are of great importance and allow the improvement of the measurement accuracy, the main requirement for obtaining high precision measurement is still an accurate calibration of the volume of the piston. In this paper a full uncertainty budget of the test rig and the methods for determining the various uncertainty contributions will be described in detail, alongside with some considerations on the implications of such a budget for the future developments of the machine.

The piston prover concept has been used for a long time now; One of the first well-documented developments of a piston prover for use as a primary standard can be found in [2], where the adaptation of a piston prover built for liquid measurements to gas measurements is described. Since then, several variants and adaptations have been developed for various applications. A recent review of piston provers used as primary standards can be found in [3], alongside with a description of their theory of operation. In [4] a large, hydraulically-driven piston prover is described, including a discussion on the dimensional analysis of the piston itself. [5] discuss the double-piston concept, which has the advantage of allowing measurements during both runs of the piston, but at the price of an increase in complexity.

In order to provide a reference frame for the present work, the metrological properties of a few test rigs developed in other NMIs, taken from the BIPM KCDB, are presented in the following Table 1:

NMI	Standard type	Range /m^3/h	Uncertainty / %
INRIM	Piston (standard described here)	1-150	0.05
INRIM	Bell	0.06-6	0.12
VSL	Bell	1-400	0.09
VSL	Piston (see also [4])	5-230	0.06 to 0.29
CMI	Bell	0.5-280	0.07

Table 1. Metrological properties of some gas flow primary standard.

This is the third INRIM work ([6], [7]) in a series of papers that aim to disseminate the knowledge of flow measurement standards focusing on a metrological point of view. Authors think that the hypotheses and the theories underlying the uncertainty budget of a standard are fundamental for the correct evaluation of its uncertainties, but often the details of this analysis are reported in languages other than English or in laboratory procedures and technical reports which are not open access. The theoretical work of uncertainty analysis must always precede the results of international comparisons which must be limited to support the validity of detailed uncertainty evaluations. It is the authors' opinion that sharing and comparing also the theoretical evaluation of the uncertainty and not only the numerical results is important. This paper has been divided in sections in order to facilitate its reading and make the analysis even clearer and therefore usable by those who do not yet have solid experience in the field of primary standards.

2. Facility and instrumentation description

2.1. The Measurement ambient

The MeGas facility is located at the gas flow laboratory in INRIM. The laboratory is temperature controlled and the temperature during calibration can be set in the range from 15 °C to 25 °C. Whenever the temperature setting is changed, at least 12 hours should be waited before taking measurements. Under normal conditions, the temperature is set to 20 °C. The relative humidity value is currently not controlled but is measured and recorded using a TESTO thermo-hygrometer data logger. The ambient pressure too is not controlled and it is determined,

with small variations, by the external atmospheric pressure and is measured by a Ruska barometer. During a single measure of a calibration, the pressure changes must be contained within ±200 Pa. If this condition is not met, the calibration is considered invalid and repeated.

2.2. The Piston Prover

The MeGas test rig described in the present paper, is a single-stroke, plunger-type piston prover. It was designed and built at the then-IMGC (now INRIM) in the mid-1980s with the aim of developing the largest piston prover that could be housed in the existing laboratory premises. The goal of the development was the reduction of one order of magnitude of the "purely volumetric" uncertainty components that affect bell provers. This was obtained by eliminating the oil bath and by adopting a rigid, precisely machined and measured body to sweep the volume, which naturally leads to the piston prover concept. The plunger type (namely a long, vertical cylindrical piston forced to sink through a gasket into a slightly larger, rigid but mechanically unfinished chamber containing the gas) was preferred over a traditional piston-cylinder system because of metrological (the external diameter can be measured more accurately than the internal one) and practical reasons (it is easier and cheaper to machine the piston than the cylinder, and the gasket is more easily accessible).

The resulting device is a structure 6 m high (Fig. 1), with at its top a platform (Fig. 1A) where a finely controlled brushless motor drives, through a gearbox, the female ball-screw of a lead screw (Fig. 1B) connected with the piston. This apparatus causes the vertical movement of the piston (Fig. 1C) and the emission of pulses from a rotating encoder (Fig. 1A) fitted on the female screw. The piston is constituted by a 1000 mm nominal diameter, 1630 mm long and 14 mm thick carbon-steel cylinder fitted to a massive bottom flange. The external surface of the cylinder is chromium plated, ground and polished. The leak-proof gasket at the top of the chamber is a Teflon-coated, 1000 mm diameter O-ring compressed to the necessary and adjustable extent by an upper flange. The internal diameter of the measurement chamber (Fig. 1D) is 1095 mm; in the clearance between its walls and the piston, 10 Platinum Resistance Temperatures (PRTs) are installed at different heights and positions in order to measure the average gas temperature and to detect possible non uniformities. The chamber rests on the 1950 mm diameter base of the prover. A bended pipe is connected to a 100 mm bore at the center of the base which conveys the gas displaced by the piston towards the test line. A group of automatically operated valves (a safety valve, one for admission of atmospheric air and one

for gas delivery to the test line) are installed at the facility exit (Fig. 1E) . The internal volume of the prover is about 1500 L when the piston is at its upper rest position; the volume of the piston is more than 1200 L, however, considering the parts of the piston stroke that must be devoted to acceleration, deceleration and the emergency stop switches installed at both ends, the largest gas volume that can be displaced and measured is about 800 L.

2.2.1 Mode of Operation

The operation of the prover is fully automated and controlled by a specific electronic apparatus, which controls the movement according to the required mode. The instrumentation – namely the encoder, the chronometer, the various transducers measuring piston velocity, displaced volume, temperatures and pressure - is interfaced to a PC for recording of the data.

The mode of operation of the piston is as follows. The piston is placed at its initial position (top or bottom depending whether supply or admission mode is required). A period of one minute is allowed for temperature stabilization, then the piston is moved at the programmed speed. After velocity and pressure stabilize, the measurement phase begins, *i.e.* the initial measurement conditions (position of the piston y_i and thermodynamic conditions p_i, T_i) are recorded, while the chronometer is started. Once the required displacement has been performed, the final measurement conditions (position of the piston y_f and thermodynamic conditions p_f, T_f) are recorded and the chronometer is stopped, providing the test time Δt; the piston is then brought to rest. The difference $\Delta y = y_f - y_i$ between the initial and final positions of the piston is the measured displacement of the piston and, when multiplied by the piston base area (which is considered as a constant, see Sec. 4), allows the computation of the displaced volume of gas ΔV. The initial and final thermodynamics conditions allow to compute the initial and final gas densities, which are used to determine the reference volume and, together with the elapsed time, the reference flow rate provided by the piston, as described in detail in Sec. 3. Depending on the working mode, supply or admission, the sign of Δy will be different; this will lead to slightly different corrections in the determination of the final values, as described in Sec. 3. It is important to notice that measurements are taken after the stabilization of the piston movement and of the pressure, *i.e.* in stationary conditions. No unsteady effects are therefore taken into account.

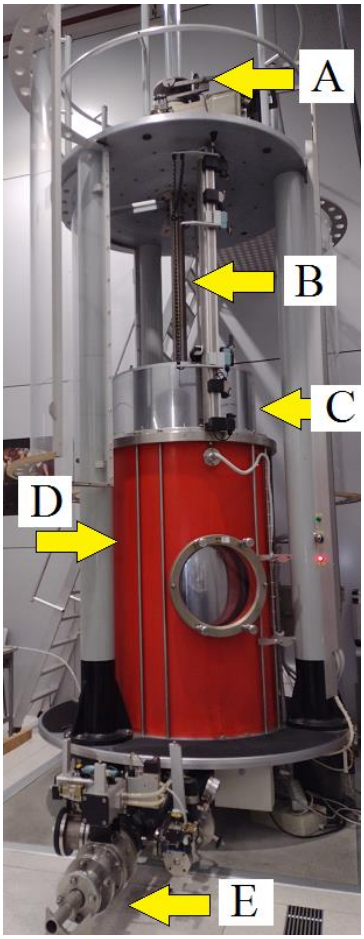

Fig. 1. MeGas Facility, A: MeGas encoder and piston control, B: screw, C: Piston, D: measurement chamber, E: facility exit

2.3. The measurement system

The traceability of the measurements carried out in the gas flow laboratory is guaranteed by the metrological chain detailed in the following traceability diagram (Fig. 2).

The traceability of the piston displacement and of the piston base area are obtained by means of the geometrical calibration of MeGas.

The traceability of the thermometric chain, the barometer and the hygrometer is guaranteed by calibration to the respective primary standards at INRIM.

Traceability of the chronometer is to the Italian National Time, as described in detail in Sec. 4.3.4.

Since this section focuses on the measurement system of the MeGas, it is important to specify that the measurement chain of MeGas during its functioning as primary standard (Sec. 2.2) does not correspond to the measurement chain used for the MeGas geometrical calibration (Sec. 4.1).

The measurement chain of the geometrical calibration of MeGas is shown in Fig. 5. During the MeGas geometrical calibration, the displacement was evaluated by an interferometric system, traceable to the INRIM primary length standard whereas the piston base area was evaluated by a couple of linear encoders that measured the diameter of the piston at different heights. The two linear encoders are traceable to the primary standard of length by calibration at INRIM.

A special, stainless steel bar traceable to the LNE primary length standard was used as reference for the linear encoders during the MeGas calibration.

The geometrical calibration of the MeGas was described in detail by three previous works [8], [9], [11]. In Sec. 4 a brief description of the geometrical calibration procedure of the MeGas is summarized in order to provide the reader with the basic elements to better understand the uncertainty analysis and the uncertainty budget.

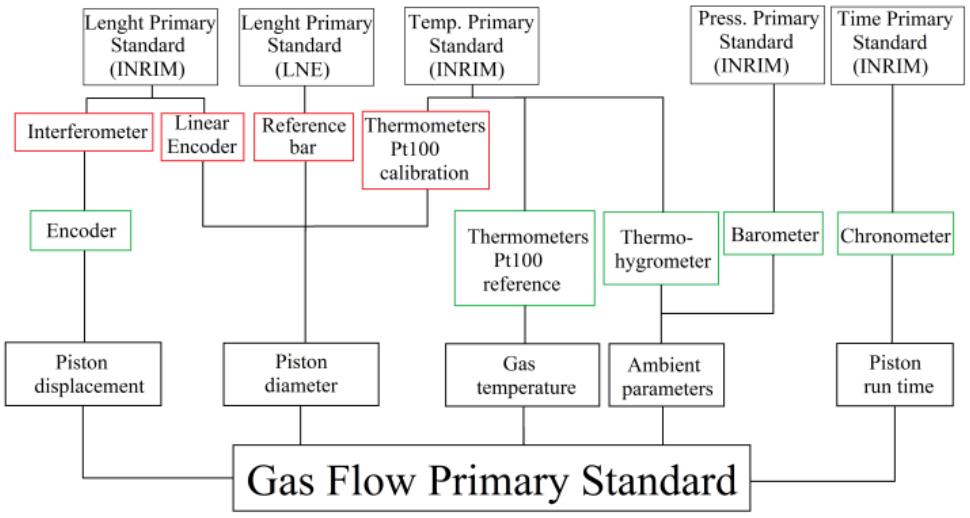

Fig. 2. Traceability diagram of MeGas. The instruments framed in red (first level line) added to the instruments framed in green (second level line) constitute the measurement chain for the MeGas calibration procedure. The instruments framed in green also constitute the in-use measurement chain of the test rig.

3. Model equation for the flow standard at MeGas

The computation of the reference volume and of the flow rate provided by the piston is done using the so-called method of the balance of mass, *i.e.* by evaluating the mass of gas delivered (or accepted) by the prover during the test. It was chosen to use this method instead of the simple determination of the volume since it allows to keep directly in consideration the variations in thermodynamic conditions for the computation of the quantity of gas that has flown through the test rig bore; additionally, the result is invariant with the thermodynamic conditions, and can therefore be readily converted to any desired form (*e.g.* molar flow, volume flow of gas at reference condition etc.); finally, the method takes directly into account the effects of compression of the dead volume, which are anyway very small due to the small overpressures within the cylinder. In Sec. 4.3.3 and 5, it will also be shown that the uncertainty associated with the measurement can be controlled with relative ease by the application of this method. The drawback of the method is that it requires measuring the initial and final thermodynamic conditions of the gas; such measurements are described in detail in Sec. 4.3.1 and 4.3.2. The displaced mass of gas ΔM is then computed as the difference between the final mass (obtained by multiplying the final density times the final volume estimate) and the initial mass (obtained by multiplying the initial density by the initial volume estimate); this difference can be rewritten as the final density by multiplying the displaced volume ΔV, computed as described in Sec. 2.2.1, with the final density and by adding a correction term which depends on the density variation and on the initial volume:

$$\Delta M = \rho_2 V_2 - \rho_1 V_1 = \rho_2 \Delta V + V_1 (\rho_2 - \rho_1) \quad (1)$$

This formulation of the equation shows that the uncertainty contribution of the initial volume is minimal (since it multiplies a value that is very small if the variation of thermodynamic conditions is small) and therefore even large uncertainties on the initial volume will affect only slightly the final result; in other words, it is not necessary to estimate the dead volume to a great accuracy, which is often difficult. ΔM can then be converted to the reference volume ΔV_{Ref} of gas – not to be confused with the displaced volume ΔV - at the specified reference conditions (which can be defined to a standard value, *e.g.* 0° C and 1 atm, or be the conditions at the Device Under Test - DUT) for comparison to the DUT output as follows:

$$\Delta V_{Ref} = \frac{\rho_2 V_2 - \rho_1 V_1}{M_{mol}} \cdot \frac{R T_{ref}}{p_{ref}} = \frac{\rho_2 \Delta V + V_1 (\rho_2 - \rho_1)}{M_{mol}} \cdot \frac{R T_{ref}}{p_{ref}} \quad (2)$$

where R is the universal gas constant, M_{mol} is the molar mass of the test gas, T_{ref} and p_{ref} are the thermodynamics conditions to be used for the conversion.

It should be noted that in writing Eq. 1 it is assumed that the final volume is larger than the initial one (admission mode) in order to have a positive value of the mass variation and therefore of the reference volume. The corresponding equation for supply mode is slightly different in that signs are opposite; this leads to small changes in the final formulation used for the computations, but the analysis of this second formulation can be performed in the same way leading to similar results (not presented here for conciseness).

The flow rate, in mass (Q_M) or volume (Q_V), is computed by dividing the computed mass or volume by test time measured by the chronometer:

$$Q_M = \frac{\rho_2 V_2 - \rho_1 V_1}{\Delta t} = \frac{\rho_2 \Delta V + V_1 (\rho_2 - \rho_1)}{\Delta t} \quad (3a)$$

$$Q_V = \frac{\rho_2 V_2 - \rho_1 V_1}{t \cdot M_{mol}} \cdot \frac{R T_{ref}}{p_{ref}} = \frac{\rho_2 \Delta V + V_1 (\rho_2 - \rho_1)}{t \cdot M_{mol}} \cdot \frac{R T_{ref}}{p_{ref}} \quad (3b)$$

Eq. 3a and Eq. 3b represent the formulation of the model equations for the computation of the flow rate delivered or accepted by the prover, while Eq. 2 is the formulation for the computation of the reference volume delivered or accepted by the prover. In the following the uncertainty analysis will be performed starting from Eq. 3b, since the corresponding analysis for Eq. 2 and Eq. 3a can readily be obtained by elimination of some terms.

4. Uncertainty analysis

The uncertainty analysis will be performed according to the document JCGM 100:2008 [10] based on Eq. 3b. The latter can be rewritten as:

$$Q_V = \frac{\Delta M}{t \cdot M_{mol}} \cdot \frac{R T_{ref}}{p_{ref}} \quad (4)$$

Eq. 4 is a multiplicative model, therefore the uncertainty associated to it can readily be obtained as:

$$\frac{u^2(Q_V)}{Q_V^2} = \frac{u^2(\Delta M)}{\Delta M^2} + \frac{u^2(t)}{t^2} + \frac{u^2(M_{mol})}{M_{mol}^2} + \frac{u^2(R)}{R^2} + \frac{u^2(T_{ref})}{T_{ref}^2} + \frac{u^2(p_{ref})}{p_{ref}^2} \quad (5)$$

The last five terms in this equation can be obtained directly as will be shown in Sec. 4.2; though, a more detailed analysis is required for the first term. In order to perform such analysis, consider again Eq. 1 in its second form. The following sensitivity coefficients can be computed:

$$\frac{\partial \Delta M}{\partial \rho_2} = \Delta V + V_1;\ \frac{\partial \Delta M}{\partial \rho_1} = -V_1;\ \frac{\partial \Delta M}{\partial \Delta V} = \rho_2\ ;\ \ \frac{\partial \Delta M}{\partial V_1} = \rho_2 - \rho_1$$

Since in Eq. 1 the quantities ρ_1 and ρ_2 are correlated, it is also necessary to consider the covariance term:

$$Cov(\rho_1, \rho_2) = \rho_0^2 \cdot \left[\frac{u^2(p_0)}{p_0^2} + \frac{u^2(T_0)}{T_0^2}\right] \quad (6)$$

Where the subscript 0 indicates the average between the corresponding initial and final quantities, under the hypothesis that variations of the thermodynamic conditions are small.

Eq. (6) was obtained by replacing the density with its expression as a function of p and T, and developing the relevant equations for covariance, by considering small variations between initial and final conditions. The sensitivity coefficient for the covariance term is:

$$\frac{\partial \Delta M}{\partial \rho_1} \cdot \frac{\partial \Delta M}{\partial \rho_2} = -V_1 \cdot (\Delta V + V_1) \quad (7)$$

It is then possible to express the absolute standard uncertainty associated to the variation of mass within the prover as follows:

$$u^2(\Delta M) = (\Delta V + V_1)^2 \cdot u^2(\rho_2) + (\rho_2)^2 \cdot u^2(\Delta V) + (\rho_2 - \rho_1)^2 \cdot u^2(V_1) + (V_1)^2 \cdot u^2(\rho_1) - 2 \cdot V_1 \cdot (\Delta V + V_1) \cdot \rho_0^2 \cdot \left[\frac{u^2(p_0)}{p_0^2} + \frac{u^2(T_0)}{T_0^2}\right] \quad (8)$$

Uncertainties associated to the densities are expressed according to their dependency on the thermodynamic conditions. After developments and simplifications, one obtains:

$$u^2(\Delta M) = \Delta V^2 \cdot \rho_0^2 \cdot \left[\frac{u^2(p_0)}{p_0^2} + \frac{u^2(T_0)}{T_0^2}\right] + \rho_0^2 \cdot u^2(\Delta V) + (\rho_2 - \rho_1)^2 \cdot u^2(V_1) \quad (9)$$

and, in relative form:

$$\frac{u^2(\Delta M)}{\Delta M^2} = \left[\frac{u^2(p_0)}{p_0^2} + \frac{u^2(T_0)}{T_0^2}\right] + \frac{u^2(\Delta V)}{\Delta V^2} + \frac{(\rho_2 - \rho_1)^2}{\rho_0^2} \cdot \frac{V_1^2}{\Delta V^2} \cdot \frac{u^2(V_1)}{V_1^2} \quad (10)$$

which can be replaced in equation (5) to give:

$$\frac{u^2(Q_V)}{Q_V^2} = \left[\frac{u^2(p_0)}{p_0^2} + \frac{u^2(T_0)}{T_0^2}\right] + \frac{u^2(\Delta V)}{\Delta V^2} + \frac{(\rho_2-\rho_1)^2}{\rho_0^2} \cdot \frac{V_1^2}{\Delta V^2} \cdot \frac{u^2(V_1)}{V_1^2} + \frac{u^2(t)}{t^2} + \frac{u^2(M_{mol})}{M_{mol}^2} + \frac{u^2(R)}{R^2} + \frac{u^2(T_{ref})}{T_{ref}^2} + \frac{u^2(p_{ref})}{p_{ref}^2}$$

(11)

Since the present paper focuses on the geometrical calibration of the piston, the uncertainty sources associated to this calibration (diameter and displacement) are discussed separately in Sec. 4.1, while sources associated to the measurement system, to the measurement technique and to the environment (instruments, ambient conditions, etc.) are discussed in Sec. 4.3.

4.1 Geometrical calibration of MeGas

The geometrical calibration of MeGas consists in the evaluation of the mean diameter of the piston and of the piston displacement (by calibrating the MeGas encoder on site) in order to make the piston diameter and displacement traceable to the primary standard of length.

The piston diameter has been evaluated by means of two linear encoders along seven generatrices of the cylindrical piston (see Fig. 3 and Fig. 4). The piston displacement has been evaluated by calibration of the encoder with an interferometer; the interferometer was placed below the MeGas base, the laser ray passing through the bore in the base providing the facility in- and outflow (see Fig. 5 and Fig. 6).

The diameter and the displacement measurement chains are acquired simultaneously according the following sequence:

1. the linear encoders are positioned on the chosen generatrix and zeroed on the reference bar;
2. the temperature inside the chamber, the pressure and humidity in the laboratory are recorded;
3. outputs from the interferometer and the linear encoders are recorded during several vertical translations (up- and downwards) of the piston; each translation is 1.28 m long with a 1 mm step, providing thus 1280 diameter measurements on each run;
4. the temperature inside the chamber, the pressure and humidity in the laboratory are recorded again;
5. after (at least) 7 repetitions the linear encoders are zeroed again; steps (1) to (4) are then repeated for another generatrix.

The piston diameter could thus be estimated as the average of 93 x 1280 diameter acquisitions.

Great care has been taken to allow the structure to settle after the operator disturbed its temperature, by monitoring the reference bar temperature and that of the air inside the cylinder.

Full details of the procedure and complete measurement results are reported in [8] and [10]. Operations necessary to prepare the MeGas facility are detailed in [9].

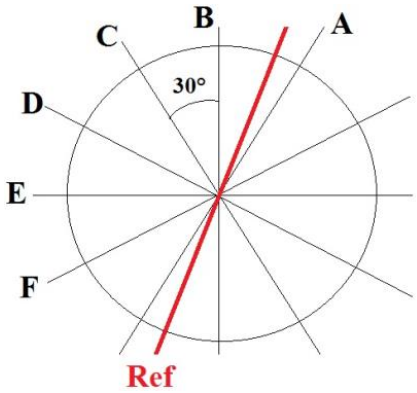

Fig. 3. Top view sketch of the piston with the positions of generatrices;

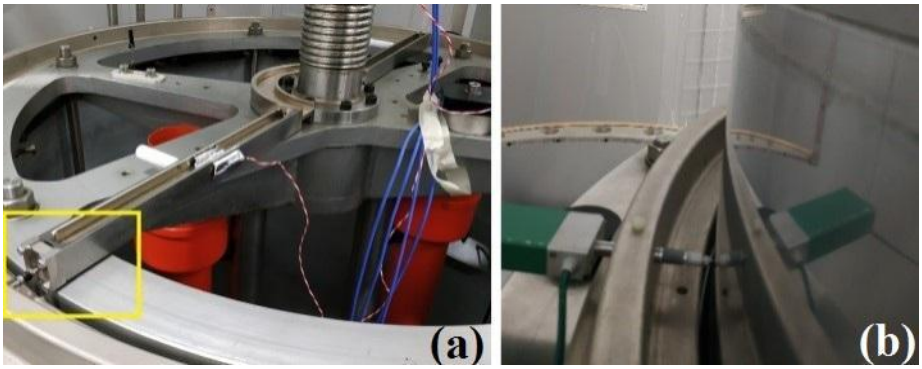

Fig. 4. (a) – Linear encoder zeroed on the reference bar (yellow frame); (b) - linear encoder during measure along one generatrix of the cylindrical piston.

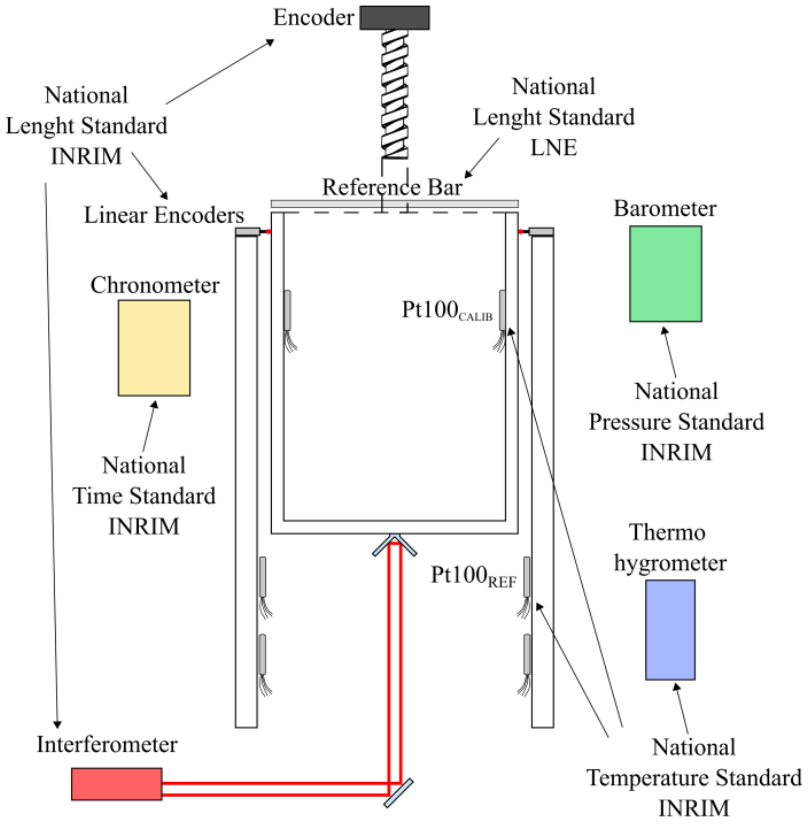

Fig. 5. Scheme of the measurement chain for MeGas, geometrical calibration

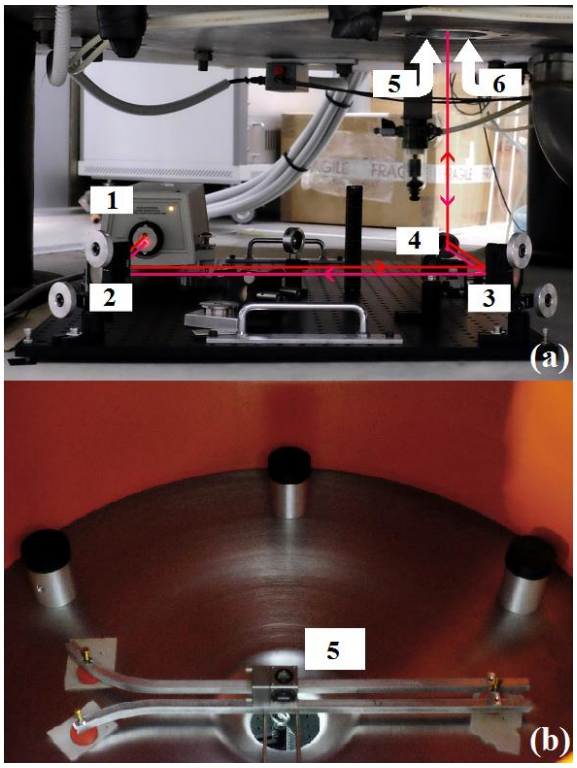

Fig. 6. (a) - Red arrows indicate the laser path. 1: interferometer, 2, 3 and 4: folding mirrors; 5: beam splitter + corner cube (visible in Fig. 6 (b)); 6: corner cube positioned on the piston inferior surface (not visible in figure); the total dead path length is of about 200 mm. (b) – 5: beam splitter + corner cube (realizing the reference arm) placed on the internal surface of the base of the chamber

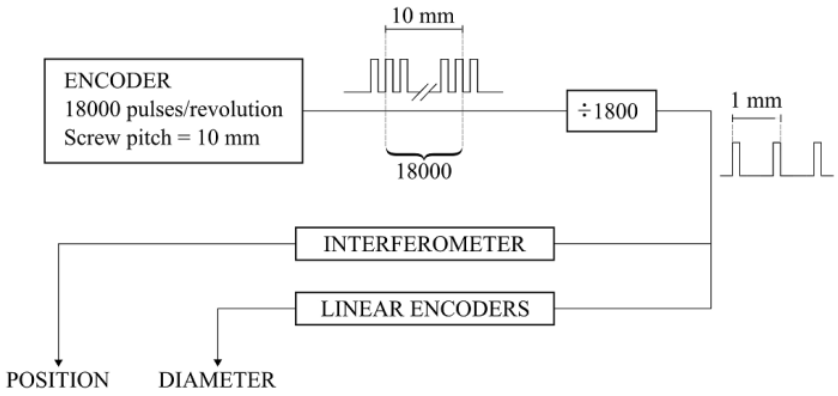

Fig. 7. Acquisition trigger block scheme.

4.1.1 Piston diameter

According to the measurement procedure applied, the diameter of a singular acquisition is evaluated as:

$$d_{i,j} = \left(\Delta L_{i,j} - \Delta L_{REF,j}\right) + L_{REF} \quad (12)$$

with i=1…1280 and j=1…93, where $\Delta L_{i,j}$ is the i-th acquisition of the j-th measure and $\Delta L_{REF,j}$ is the corresponding reference output obtained as the mean value of the measurements results ($\Delta L_{REF,1,j}$ and $\Delta L_{REF,2,j}$) obtained at different times (see point 1 and point 5 in the action list of Sec. 4.1) . The value of the reference bar is given by means of the reference bar calibration certificate The corresponding value in the most recent certificate by LNE is:

$$L_{REF} = (0.999252 \pm 0.000005) \text{ m} \quad (13)$$

The mean diameter over the 1280 acquisitions for the j-th measure is:

$$\underline{d_j} = \underline{\Delta L_j} - \Delta L_{REF,j} + L_{REF} \quad (14)$$

Finally, the mean diameter of the piston over the 93 measures is computed as:

$$\underline{d} = \frac{1}{93} \cdot \sum_{j=1}^{93} \underline{d_j} \quad (15)$$

The uncertainty associated to the single acquisition of the diameter, corresponding to the uncertainty of the measurement chain (Type B uncertainty), can be computed as:

$$u\left(d_{i,j}\right) = \sqrt{u_{CERT}^2(\Delta L) + u_{RES}^2(\Delta L) + u^2\left(\Delta L_{REF,j}\right) + u^2(L_{REF})} \quad (16)$$

where the value $u_{CERT}(\Delta L)$ is derived from the calibration certificate of the linear encoders, the value $u_{RES}(\Delta L)$ is associated to the linear encoders resolution, the value $u(\Delta L_{REF,j})$ is associated to the encoder zeroing on the reference bar and finally the standard uncertainty $u(L_{REF})$ is derived from the reference bar calibration certificate.

Each linear encoder was calibrated in INRIM. The uncertainty associated with each linear encoder was assessed by assuming a rectangular distribution with a semi-amplitude equal to the maximum correction of the reading which has to be applied according to the certificate. The uncertainty associated with the certificate $u_{CERT}(\Delta L)$ is the sum of the uncertainties associated to each encoder and the uncertainty associated with corrections, giving:

$u_{CERT}(\Delta L) = 2.19 \cdot 10^{-6}$ m.

The uncertainty associated to linear encoder resolution has been estimated to be $u_{RIS}(\Delta L) \approx 3 \cdot 10^{-8}$.

The uncertainty associate to the zeroing of the linear encoder system on the reference bar is computed assuming a rectangular distribution over the two measured values for each j-th measure:

$$u(\Delta L_{REF,j}) = \sqrt{\frac{(\Delta L_{REF,1,j} - \Delta L_{REF,2,j})^2}{12}} \quad (17)$$

and its numerical value is found to be 1.5 μm approximately. With the value of $u(L_{REF}) = 5\ \mu m$ as reported on the calibration certificate of the reference bar, the uncertainty associated to the mean diameter of the j-th measure is evaluated as:

$$u(\underline{d_j}) = \sqrt{\sigma^2(\underline{d_j}) + u^2(d_{i,j})} \quad (18)$$

where $u(d_{i,j}) = 5.7 \cdot 10^{-6}\ \boldsymbol{m}$ according to Eq. 16 and the value of $\sigma\ (\underline{d_j})$ varies from $2.0 \cdot 10^{-6}\ \boldsymbol{m}$ to $3.4 \cdot 10^{-6}\ \boldsymbol{m}$ among all the 93 measurement distributions.

The standard deviation of mean diameter calculated from the 7 generatrices (see Table 2) is $\sigma\ (\underline{d}) = 2 \cdot 10^{-5}\ m$

The mean diameter uncertainty is calculated, similarly to Eq. 18, as:

$$u(\underline{d}) = \sqrt{\sigma^2\ (\underline{d}) + u^2(d_{i,j})}\ =\ 2.1 \cdot 10^{-5}\ m \quad (19)$$

The mean diameter in the working range was therefore evaluated to be equal to:

$$\underline{d} = 0.99950\ \pm\ 4.2 \cdot 10^{-5}\ \boldsymbol{m} \quad (20)$$

In Fig. 8 and Fig. 9 the mean diameter for each generatrix and the overall mean diameter are shown.

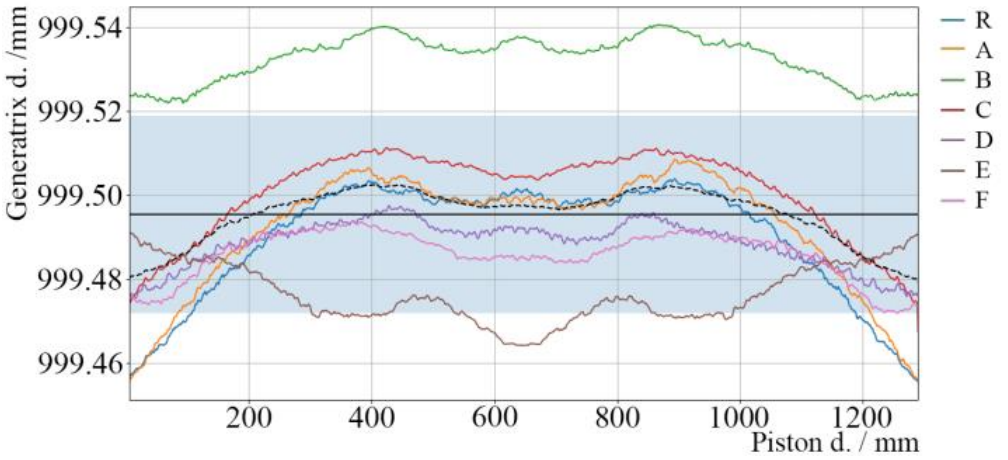

Fig. 8. Piston full travel: mean diameter for each generatrix (in color) and mean of the means (dashed black) as a function of piston displacement for the piston full travel. The continuous black line represents the mean over the piston full travel, with its standard deviation indicated by the colored area.

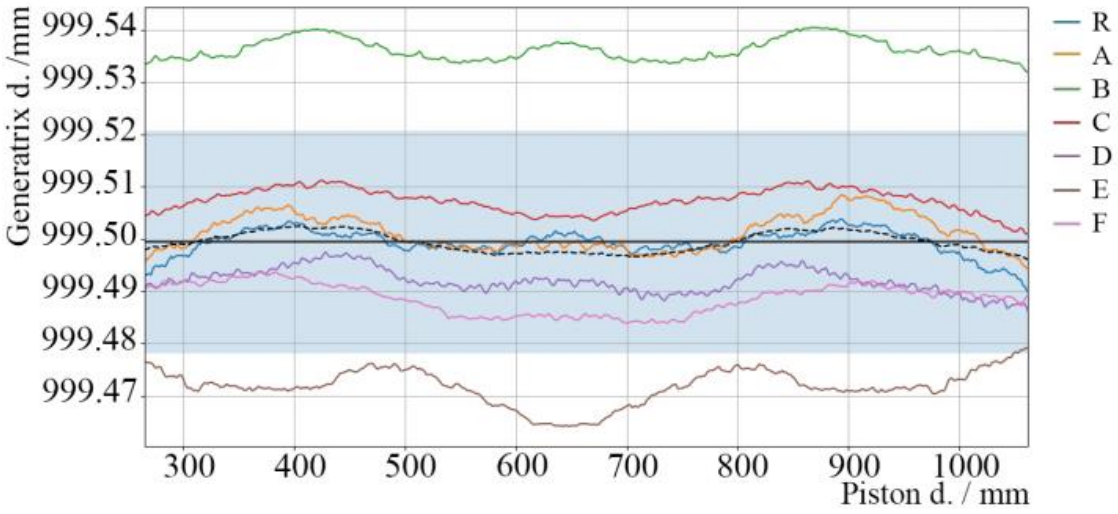

Fig. 9. Piston working range: mean diameter for each generatrix (in color) and mean of the means (dashed black) as a function of piston displacement for the piston displacement limited to the working range The continuous black line represents the mean over the piston, with its standard deviation indicated by the colored area.

The mean diameter for each generatrix is tabulated below; the mean diameter and its standard deviation are also shown.

generatrix	$\underline{d_j}$ **/ m**
R	**0.999496**
A	**0.999498**
B	**0.999533**
C	**0.999504**
D	**0.999489**
E	**0.999469**
F	**0.999486**
$\underline{\boldsymbol{d}}$ **= 0.99950 m and** $\sigma\left(\underline{\boldsymbol{d}}\right) = 2 \cdot 10^{-5}$ **m**	

Table 2. Mean diameter $\underline{d_j}$ for each generatrix and mean diameter of the piston $\underline{\boldsymbol{d}}$

4.1.2 Piston displacement

In an interferometric measure, the displacement L of an object is obtained by multiplying the number of fringes N by half the wavelength λ of the laser used.

$$L = N \cdot \frac{\lambda}{2} \tag{21}$$

In order to obtain the actual displacement L of the piston a correction factor for the vacuum wavelength and for the refractive index has to be applied to the interferometer output L_{interf}. The actual displacement L is therefore computed as:

$$L = L_{interf} \cdot \frac{\lambda_0}{\lambda_{0,interf}} \cdot \frac{n_{interf}}{n} \tag{22}$$

where λ_0 is the laser vacuum wavelength obtained from the calibration certificate, $\lambda_{0,interf}$ and n_{interf} are the vacuum wavelength and the refractive index used by the interferometer electronics for the computation of L_{interf}, which is a function of $\lambda_{0,interf}$ and n_{interf}; the refractive index n is calculated using the Edlén formula as given in Appendix A-IV of the Engineering Metrology Toolbox of NIST, Eq. A49 [12] and recalled in Eq. 23 for clearness, where T, p and RH are, respectively, the values of temperature, pressure and relative humidity during the measurement, obtained as the respective means of the initial ($T_{in,j}$, $p_{in,j}$, $RH_{in,j}$) and the final conditions ($T_{fin,j}$, $p_{fin,j}$, $RH_{fin,j}$) for every travel j=1…93 of the piston.

$$n(\lambda_0, T, p, RH) = n_{tp}(\lambda_0, T, p) - 10^{-10} \cdot p_V(RH, T) \cdot 292.75 \cdot \frac{3.7345 - 0.0401 \cdot S(\lambda_0)}{T + 273.15} \tag{23}$$

Authors decided to not add further details in this work about the computation of the refractive index n because it is a too much specific dimensional metrology topic. However, all details on the computation of n can be found in [11], [12] and [13].

According the Eq. 22, the displacement $L_{i,j}$ for a single acquisition can be calculated as:

$$L_{i,j} = L_{i,j,interf} \cdot \frac{\lambda_0}{\lambda_{0,interf}} \cdot \frac{n_{interf}}{n_{i,j}} \tag{24}$$

with *i*=1…1280 and *j*=1…93. Actually, the difference $\delta L_j = L_{i+1,j} - L_{i,j}$between two consecutive displacements is more useful for MeGas calibration purposes. As for the diameter evaluation, it has been considered the average difference for the j-th measure:

$$\underline{\delta L_j} = \frac{1}{1279} \cdot \sum_{i=1}^{1279} \quad (L_{i+1,j} - L_{i,j})$$

(25)

The average difference over the 93 measurements is computed:

$$\underline{\delta L} = \frac{1}{93} \cdot \sum_{j=1}^{93} \quad \underline{\delta L_j} \tag{26}$$

The uncertainty associated to the $\underline{\delta L}$ has been obtained as the sum of squares of its type A and type B uncertainty contributions:

$$u(\underline{\delta L}) = \sqrt{{u_A}^2(\underline{\delta L}) + {u_B}^2(\underline{\delta L})} \tag{27}$$

where:

$$u_A(\underline{\delta L}) = \sigma_{MAX}(\underline{\delta L_j}) \tag{28}$$

and

$$u_B(\underline{\delta L}) = u_B(\underline{\delta L_j})|_{j=1\ldots93} = \delta L_{interf} \cdot \frac{\lambda_0}{\lambda_{0,interf}} \cdot \frac{n_{interf}}{n} \cdot \sqrt{\frac{u^2(\delta L_{interf})}{{\delta L_{interf}}^2} + \frac{u^2(\lambda_0)}{{\lambda_0}^2} + \frac{u^2(n)}{n^2}} \tag{29}$$

The quantities $\lambda_{0,interf}$ and n_{interf}, used by the electronics of the interferometer, are considered two constants and therefore without uncertainty. The uncertainty associated to the displacement measure δL_{interf}, has been calculated with the usual propagation formula:

$$u(\delta L_{interf}) = \sqrt{u^2(\delta L_{interf,cos}) + u^2(\delta L_{interf,Abbe}) + u^2(\delta L_{interf,dp})}$$

(30)

where $u(\delta L_{interf,cos})$ is the uncertainty associated to the cosine error, $u(\delta L_{interf,Abbe})$ is the uncertainty associated to the Abbe error and $u(\delta L_{interf,dp})$ is the uncertainty associated with the dead path. The contribution due to the interferometer resolution has been considered negligible.

The errors (cosine, Abbe and dead path) were assumed equal to zero and their contributions were taken into account by including them into the uncertainty computation.

The uncertainty associated with the cosine error has been evaluated from a rectangular PDF whose amplitude is the estimation of the maximum allowed misalignment of the laser beam, obtained by applying a safety factor greater than 10 to the maximum misalignment of the laser beam estimated by using an electronic position sensor.

The uncertainty associated with the Abbe error has been evaluated from the quality of the piston manufacturing (motion-measurement axes translation) and the maximum "reasonable" rotation and assuming, again, a rectangular PDF.

The uncertainty associated with the dead path error has been evaluated from an estimate of the maximum refractive index variation in the dead path, and assuming a rectangular PDF of equal amplitude.

Further details of the three contributions in Eq. 30 can be found in [8] and [11].

The results of this analysis are summarized in Table 3.

The second uncertainty contribution in Eq. 29, namely $u(\lambda_0)$, is derived from the calibration certificate of the interferometer and is equal to $u(\lambda_0) = 1.5 \cdot 10^{-15}$ m.

Finally the uncertainty associated with the refractive index u(n) has been evaluated from the Edlen empirical formula (Eq. 23) used for the computation of the refractive index n. In particular, the uncertainty associated to the refractive index n is calculated with the following propagation formula:

$$u(n) = \sqrt{\left(\frac{\partial n}{\partial \lambda_0}\right)^2 \cdot u^2(\lambda_0) + \left(\frac{\partial n}{\partial t}\right)^2 \cdot u^2(T) + \left(\frac{\partial n}{\partial p}\right)^2 \cdot u^2(p) + \left(\frac{\partial n}{\partial RH}\right)^2 \cdot u^2(RH)} \quad (31)$$

The first term $u(\lambda_0)$ has already been described, the second, third and fourths terms are due to the ambient parameters (T, p and RH) variation during the measurement.

The evaluation of the uncertainty of these three terms is not reported here. An example of values obtained by the ambient parameters uncertainty analysis follows in Table 4 and are obtained taking into account: the resolution of the instruments, their accuracy, the calibration certificate of the instruments and the standard deviation of the acquired samples. The example in Table 4 reports the computation of the reflective index uncertainty u(n) by means of the maximum standard uncertainty evaluated for every environmental parameter during all the measurements periods. During the 15-day measurement session, the average uncertainties in the refractive index were $u(n)_{average} = 3.68 \cdot 10^{-8}$

with a peak-peak variation of $u(n)_{max} = 4.76 \cdot 10^{-8}$. The value $u(n)_{average}$ is used for the final computation of uncertainty associated to the piston displacement.

Finally, the uncertainty associated to the piston displacement $\underline{\delta L}$ can be computed according to Eq. 27 as follow:

$$u(\underline{\delta L}) = \sqrt{{\sigma_{MAX}}^2(\underline{\delta L_j}) + \left(\delta L_{interf} \cdot \frac{\lambda_0}{\lambda_{0,interf}} \cdot \frac{n_{interf}}{n}\right)^2 \cdot \left(\frac{u^2(\delta L_{interf})}{{\delta L_{interf}}^2} + \frac{u^2(\lambda_0)}{{\lambda_0}^2} + \frac{u^2(n)}{n^2}\right)} \quad (32)$$

$u(\underline{\delta L}) = 1.4 \cdot 10^{-6}$ m.

Table 5 summarizes the value of contributions expressed in Eq. 32.

For the MeGas functioning it is necessary to estimate the displacement of the piston by means of the facility encoder and not by means of the interferometer that is used only during the procedure of the geometrical calibration of the piston. To do this the transfer function of the encoder (ERA180 Heidenain, with a resolution of 18000 pulse per round) is applied to the encoder output itself:

$$\delta L_{trans\_funct.} = \left(\frac{1}{1800} \cdot N_{enc}\right) \cdot 1 \cdot 10^{-3}\text{m} \quad (33)$$

where N_{enc} is the number of pulses output of the MeGas encoder for a displacement δL of the piston. Finally, according to the reported analysis, the mean displacement of the piston evaluated taking into account the encoder transfer function was found to be:

$$\underline{\delta L} = \left(\frac{1}{1800} \cdot N_{enc}\right) \pm 2.8 \cdot 10^{-6}\text{ m} \quad (34)$$

Fig. 10 shows a detail of the step size variation caused by the screw pitch.

Standard uncertainty	**Probability Density Function**
$u(\delta L_{interf,cos})$= 3·10-8 m	rectangular
$u(\delta L_{interf,Abbe})$= 5.8·10-7 m	rectangular
$u(\delta L_{interf,dp})$= 1.2·10-8 m	rectangular
$u(\delta L_{interf})$= 5.8·10-7 m	

Table 3. Contributions of uncertainty associated to the measured displacement δL_{interf}.

Standard Uncertainty	**Probability Density Function**
$u(\lambda_0)$= 1.5·10^{-15} m	normal
$u(T)_{max}$= 0.02 K; $u(t)_{max}$ = 0.02 °C	normal
$u(p)_{max}$= 4.30 Pa	normal
$u(RH)_{max}$=1.75%	normal
Sensibility Coefficient (typical value)	
$\frac{\partial n}{\partial \lambda_0}$=-1.2·10^{-8} nm^{-1}	$\frac{\partial n}{\partial p}$=2.5·10^{-9} Pa^{-1}
$\frac{\partial n}{\partial t}$=-1·10^{-6} K^{-1}	$\frac{\partial n}{\partial RH}$=-2·10^{-8}
$u(n)$ = **2.27·10^{-8}**	

Table 4. Example of computation of uncertainty associated to the refractive index $u(n)$.

Standard uncertainty	**Probability density function**
$\sigma_{MAX}(\underline{\delta L_j})$= 1.2·10^{-6} m	normal
$u(\delta L_{interf})$= 5.8·10^{-7} m	rectangular
$u(\lambda_0)$= 1.5·10^{-15} m	normal
$u(n) = u(n)_{average}$= 3.68·10^{-8}	rectangular
$u(\underline{\delta L}) = 1.4\ \mu m$	

Table 5. Contributions of uncertainty associated to the piston displacement.

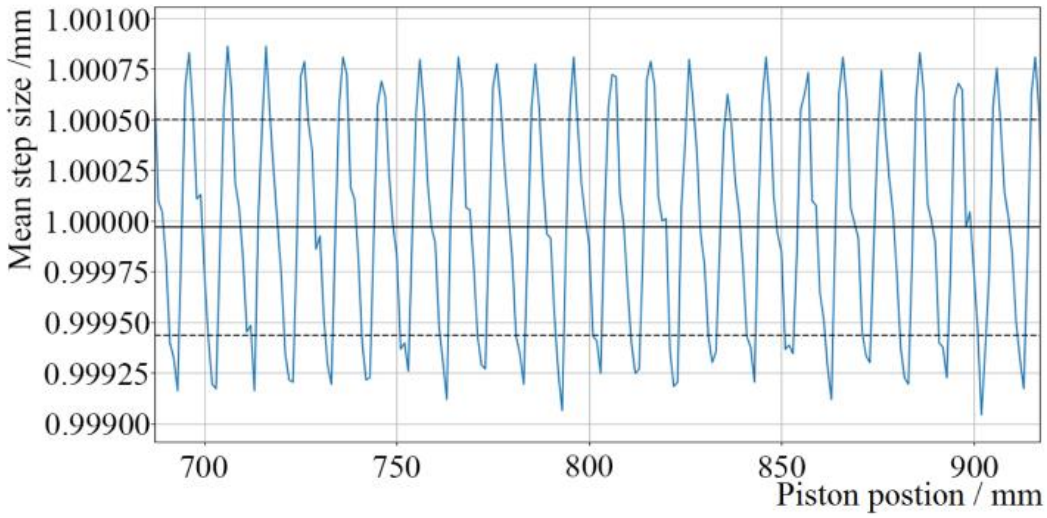

Fig. 10. Mean step size as a function of piston displacement over a portion of its travel. The continuous black line is the mean step over the piston travel range, the dashed lines indicates its standard deviation, showing the step size variation caused by the screw pitch.

As a comparison, the calibration performed in 1999 provided a mean diameter of 999.51 mm with an associated uncertainty of 0.02 mm, and the uncertainty associated to the displacement reading performed by the encoder was found to be 1,5 μm

4.2 Displaced Volume Uncertainty

As described in Sec. 2.2.1, the (nominal) volume of gas displaced by the piston can be computed from the piston displacement and its section (obtained from the diameter):

$$\Delta V = \underline{\delta L} \cdot \pi \left(\frac{\underline{d}}{2}\right)^2 \tag{35}$$

Eq. 35 is a simple multiplicative model, therefore its uncertainty can be easily obtained applying the usual formulations for this type of models [10]:

$$\frac{u(\Delta V)}{\Delta V} = \sqrt{\left(\frac{u(\underline{\delta L})}{\underline{\delta L}}\right)^2 + 2 \cdot \left(\frac{u(\underline{d})}{\underline{d}}\right)^2} \tag{36}$$

Furthermore, an uncertainty term associated to possible in-use thermal deformations of the driving screw $\left(\frac{u(\Delta V)}{\Delta V}\right)_{T,S}$ was evaluated. Considering the maximum temperature variations described earlier, this term was evaluated to a relative value of 0.00036% (*i.e.* $\left(\frac{u(\Delta V)}{\Delta V}\right)_{T,S} = 0.0000036$), which will be added in quadrature to equation (36) to give:

$$\frac{u(\Delta V)}{\Delta V} = \sqrt{\left(\frac{u(\underline{\delta L})}{\underline{\delta L}}\right)^2 + 2 \cdot \left(\frac{u(\underline{d})}{\underline{d}}\right)^2 + \left[\left(\frac{u(\Delta V)}{\Delta V}\right)_{T,S}\right]^2} \quad (37)$$

Substituting the values obtained in Sec. 4.1.1. and Sec. 4.1.2, one will obtain that the uncertainty on the displaced volume is composed by two essentially constant terms, and by a term whose value is reduced as the piston displacement increases. It will be therefore possible to limit the overall uncertainty by increasing the piston displacement, which is the reason why MeGas procedures prescribe a minimum volume (*i.e.* a minimum displacement) for calibrations.

Table 6 reports an example of evaluation of the uncertainty associated with the displaced volume u(ΔV) in the case of ΔV=50 L and ΔV=100 L. It can be observed in Table 6 that the displaced volume relative uncertainty u(ΔV)/ ΔV is a decreasing function of the displacement alone under the assumptions discussed in the present paper. Additionally, it can be seen that, for such values of the displacement, the uncertainty components associated to the piston diameter and displacement are of the same order of magnitude.

ΔV=50 L	
Standard uncertainty	**Probability density function**
$\frac{u(\underline{\delta L})}{\underline{\delta L}} = \ 2.197 \cdot 10^{-5}$	Rectangular
$\frac{u(\underline{d})}{\underline{d}} = 2.1 \cdot 10^{-5}$	Normal
$\left(\frac{u(\Delta V)}{\Delta V}\right)_{T,S} = 3.6 \cdot 10^{-6}$	Rectangular
$\frac{u(\Delta V)}{\Delta V} = 3.71 \cdot 10^{-5} \quad \rightarrow \quad u(\Delta V) = 1.86 \ \cdot 10^{-3} L$	
ΔV=100 L	
Standard uncertainty	**Probability density function**
$\frac{u(\underline{\delta L})}{\underline{\delta L}} = \ 1.098 \cdot 10^{-5}$	Rectangular
$\frac{u(\underline{d})}{\underline{d}} = 2.1 \cdot 10^{-5}$	Normal
$\left(\frac{u(\Delta V)}{\Delta V}\right)_{T,S} = 3.6 \cdot 10^{-6}$	Rectangular
$\frac{u(\Delta V)}{\Delta V} = \ 3.19 \cdot 10^{-5} \quad \rightarrow \quad u(\Delta V) = 3.19 \cdot 10^{-3} \ L$	

Table 6. Example of uncertainties computation for a nominal displaced volume of 50 L (corresponding to a piston displacement of about 63.7 mm) compared to a nominal displacement volume of 100 L (corresponding to a piston displacement of approximately 127 mm)

4.3 Other Uncertainty Sources

Considering again Eq. 11, it can be observed that several components influence the final result in addition to the uncertainty associated with the measured volume. The following subsections are dedicated to the analysis of such components.

4.3.1 Pressure measurement

Pressures are measured using a barometer traceable to the Italian National Pressure Standard; the standard uncertainty associated to the barometer is obtained by considering the calibration uncertainty, taken directly from the relevant calibration certificate, the standard deviation of the calibration coefficient at the various calibration pressures, and the drift uncertainty, which is estimated based on the historical series of calibrations. Since the two pressure measurements are strongly correlated because they are performed through the same instrument, the uncertainty associated with their average can be considered equal to the average of their uncertainties, *i.e.* essentially the uncertainty associated with each measurement. As an example, data from the certificate presently used provide an overall standard uncertainty of 2.82 Pa, approximated to 3 Pa; the pressure within the prover can be considered constant since the piston movement is sufficiently slow to rule out any dynamic pressure variations. Since the operating pressure of the piston is essentially the ambient pressure, which at the elevation of the laboratory is on average of about 98 kPa, it can be stated that $\frac{u(p_0)}{p_0} = \frac{3}{98000} = 3.1 \cdot 10^{-5}$

4.3.2 Temperature measurement

Temperature within the chamber is measured using a set of 8 PT100 probes traceable to the Italian National Temperature Standard, positioned within the chamber; in particular, one of the probes stands 5 cm over the bore for gas exit, while the other 7 are placed within the gap between the piston and the chamber along three circumferences at different heights spanning most of the chamber height. By considering the calibration uncertainty and the estimated drift uncertainty, the total uncertainty associated to a single probe (PT100) is 0.01 K. The size of the chamber is quite large, therefore spatial variations of temperature are possible, albeit they will be mitigated by the mixing induced by the piston movements and by the fact that the temperature in the room is controlled as described earlier; the measurements performed with the 8 probes allow to determine an average temperature within the chamber, whose uncertainty can be evaluated as the standard deviation of the values measured by the different probes, and is computed

at every temperature measurement (initial and final); a typical value for this contribution is of 0.02 K; this low value is justified by the mitigating effects described earlier. The composition in quadrature of the probes' uncertainties and of the averaging uncertainty leads to a (typical) value of 0.0223 K, approximated to 0.025 K, and therefore, considering a typical working temperature of 20 °C (293.15 K), it comes out that

$$\frac{u(T\ )}{T} = \frac{0.025}{293.15} = 8.5\ \cdot 10^{-5}$$

4.3.3 Initial volume estimate

The initial volume of the measurement is evaluated by adding the dead volume estimate to the currently measured displaced volume. The dead volume is estimated through geometrical computations based on the design dimensions of the piston and the cylinder; the relative standard uncertainty associated with this value is estimated to be of about 3% of the dead volume. Since the relative uncertainty associated with the measurement of the displaced volume is far smaller than this value, it can be considered that the relative uncertainty of the initial volume corresponds to the relative uncertainty associated with the dead volume. Notice that applying the estimate for the relative uncertainty of the dead volume to the whole initial volume provides an estimate which is more and more detrimental as the piston rises within the prover. Though, due to the very small sensitivity coefficient associated with the initial volume (see Sec. 4 for details and Table 7 for an example), this does not substantially impact the final uncertainty estimate of the whole test rig.

4.3.4 Time measurement

Time is measured through a quartz chronometer included in the control system of the test rig; this chronometer is periodically checked against a precision chronometer traceable to the Italian National Time Standard. The uncertainty associated to the quartz chronometer due to this checking procedure is estimated precautionary to 1 ms; dividing this value by the minimum test time of 60 s, one gets for the maximum value of the time uncertainty:

$$\frac{u(t)}{t} = \frac{0.001}{60} = 1.7 \cdot 10^{-5}$$

4.3.5 Gas Properties Estimate

The gas properties M_{mol} and R are obtained from suitable databases; in particular, as of the present date, the molar mass, together with its uncertainty, is obtained from the IUPAC Technical Report [14]; as an example, when pure molecular nitrogen (N_2) is used, such tables provide $M_{mol} = 28.013710 \pm 0.00085$, *i.e.* a relative uncertainty of 0.003%. The gas composition is not considered as a possible source of uncertainty in the case of pure gases (which is the case considered for the definition of the CMC) since the laboratory uses gas with purity of at least 5.5 (99.9995% pure). Regarding the molar gas constant R, this value is taken from the CODATA recommended values list maintained by NIST [9]; since the 2018 revision, this value is considered as exact and therefore not affected by uncertainty.

4.3.6 Reference Conditions

The reference conditions used for the normalization of the results can have two sources, depending on the application. In the simplest case, such conditions are standardized conditions, therefore they are exact values not affected by any uncertainty; in this case the last two terms in Eq. 11 are zero. Notice, though, that in this case an additional uncertainty term associated with the method used by the DUT for the normalization of its output to the same reference conditions must be evaluated, but this is outside the scope of the present paper. On the other hand, if the reference conditions are defined as the ones at the DUT, the last two terms of Eq. 11 correspond to the uncertainty associated to the measurement of such conditions, which can be measured either by instruments associated to the DUT itself, or by the instrumentation available to the laboratory. In both cases, the evaluation of these terms is performed in the same way as discussed in Sec. 4.3.1 and Sec. 4.3.2 by replacing the values indicated there with the corresponding values of the employed instrumentation and the estimate for the fluctuation of the thermodynamic conditions at the DUT.

4.3.7 Leaks

The presence of leaks from the machine openings is periodically checked by creating a pressure differential with the ambient equal to the maximum operating pressure of the piston; the pressure within the piston is then monitored for at least one hour to check for possible deviations, while checking the corresponding temperature variations and compensating for them; experimental results show that leakages from the piston are negligible.

4.3.8 Compressibility factor Z

Possible deviations of the gas behavior from the ideal gas law, which is assumed in the evaluation of the densities, were considered by computing the variations of the compressibility factor Z in the case of pure nitrogen (typically used in the test rig) through the software REFPROP Mini by NIST [15]; the results show that for a variation of 2000 Pa and 0.2 K (which are well beyond the admissible variations of conditions within the prover during one test, but might represent the difference between conditions in the test rig and at the DUT in unfavorable conditions) the variation of the compressibility factor is within 7 parts per million; since this value is largely smaller than other uncertainty components, it is considered as negligible.

5. Uncertainty budget

This section summarizes the different uncertainty contributions to define the uncertainty budget associated with the primary gas flow standard at MeGas.

The gas flow is computed according to Eq. 11 here reported for the reader.

$$\frac{u^2(Q_V)}{Q_V^2} = \left[\frac{u^2(p_0)}{p_0^2} + \frac{u^2(T_0)}{T_0^2}\right] + \frac{u^2(\Delta V)}{\Delta V^2} + \frac{(\rho_2-\rho_1)^2}{\rho_0^2}\cdot\frac{V_1^2}{\Delta V^2}\cdot\frac{u^2(V_1)}{V_1^2} + \frac{u^2(t)}{t^2} + \frac{u^2(M_{mol})}{M_{mol}^2} + \frac{u^2(R)}{R^2} + \frac{u^2(T_{ref})}{T_{ref}^2} + \frac{u^2(p_{ref})}{p_{ref}^2}$$

Table 7 shows an example of uncertainty budget in case of following typical conditions:

$p_{ref} = p_o = 98000$ Pa, $T_{ref} = T_0 = 293.15$, $\Delta V = 100$ L, $V_1 = 800$ L, flow rate = 100 L/min, measurement time = 1 min and a variation of p and T conditions of about 20 Pa and 0.1 K between the initial conditions and the final conditions of measurement corresponding for this example to: $p_1 = 97990$ Pa, $p_2 = 98010$ Pa, $T_1 = 293.10$ K, $T_2 = 293.20$ k, $\rho_0 = 1.126135$ kg/m^3 $\rho_1 = 1.12621$ kg/m^3, $\rho_2 = 1.12606$ kg/m^3.

Relative uncertainty	Probability density function	Sensitivity coefficient	Contribution	Relative weight (%)
$\frac{u(p_0)}{p_0} = \frac{3}{98000} = 3.1 \cdot 10^{-5}$	Normal	1	$9.61 \cdot 10^{-10}$	4.9
$\frac{u(T_0)}{T_0} = \frac{0.025}{293.15} = 8.5 \cdot 10^{-5}$	Normal	1	$7.225 \cdot 10^{-9}$	37.0
$\frac{u(\Delta V)}{\Delta V} = 3.19 \cdot 10^{-5}$	Normal	1	$9.61 \cdot 10^{-10}$	4.9
$\frac{u(V_1)}{V_1} = 3.0 \cdot 10^{-2}$	Rectangular	$1.1355 \cdot 10^{-6}$	$1.022 \cdot 10^{-9}$	5.2
$\frac{u(t)}{t} = \frac{0.001}{60} = 1.7 \cdot 10^{-5}$	Rectangular	1	$2.89 \cdot 10^{-10}$	1.5
$\frac{u(M_{mol})}{M_{mol}} = 3.0 \cdot 10^{-5}$	Normal	1	$9.00 \cdot 10^{-10}$	4.6
$\frac{u(R)}{R} = 0 \ (exact\ value)$	---	-	-	-
$\frac{u(T_{ref})}{T_{ref}} = \frac{u(T_0)}{T_0} = 8.5 \cdot 10^{-5}$	Normal	1	$7.225 \cdot 10^{-9}$	37.0
$\frac{u(p_{ref})}{p_{ref}} = \frac{u(p_0)}{p_0} = 3.1 \cdot 10^{-5}$	Normal	1	$9.61 \cdot 10^{-10}$	4.9
$\frac{u(Q_V)}{Q_V} = 1.40 \cdot 10^{-4}$				

Table 7. Example of computation of the relative uncertainty of the gas flow at the MeGas primary standard.

It can be observed that the main contributions to the overall uncertainty are the ones associated with the temperature measurement, as could be expected. It is also to be noticed that the other contributions, and in particular the two associated to volume measurement, have approximately the same magnitude.

Q / L/min	ΔV /L	**t / min**	$\frac{u(Q_V)}{Q_V}$ / -
100	**100**	**1**	$1.40 \cdot 10^{-4}$
50	**50**	**1**	$1.41 \cdot 10^{-4}$
10	**10**	**1**	$1.78 \cdot 10^{-4}$
1	**1**	**1**	$1.11 \cdot 10^{-3}$
1	**50**	**50**	$1.40 \cdot 10^{-4}$

Table 8. Computation of the relative uncertainty of the gas flow at the MeGas primary standard for five representative cases, at the same condition of Table 7

It can be observed that, as the delivered volume decreases, the uncertainty associated with the flow rate increases, and quite dramatically for very low volumes. This is the reason why MeGas procedures prescribe a minimum delivered volume of 50 L for measurements. It can be noticed by comparing the second and the last row that also the measurement time has an influence, but similar computations show that this effect is very small for measurement times larger than one minute, which is why MeGas procedures also prescribe a minimum measurement time of 60 s. The results discussed in the present article will be of course validated through appropriate International Comparisons; one of these comparisons is currently underway, and INRIM already performed its set of measurements, although results are not yet available.

6. Conclusions

This paper presents a complete analysis of the measurement capabilities of the MeGas gas flow standard including uncertainty. Its features, traceability chain and the uncertainty budget of the measurements it can perform have been described in detail. Special attention has been dedicated to the dimensional calibration of the piston diameter and displacement. The values obtained from this calibration are in good agreement with the one that was carried out at the piston initial installation in 1999, thus confirming the stability of the standard. This work supports the uncertainties claimed by INRIM but, above all, provides a useful guide for a study of the uncertainty associated with a general

piston proper gas flow standard. International comparisons are certainly a fundamental exercise for confirming or not the measurement capabilities of a standard, but in the event that the comparison has not been concluded successfully, the results of comparison do not provide a certain indication of what the error may be in assessing the uncertainty of the sample compared. Providing the uncertainty budget details of a primary gas flow standard can therefore be a valid tool to allow a theoretical comparison of standard as well.

References

[1] G. Cignolo, A. Rivetti, G. Martini, F. Alasia, G. Birello, G. La Piana, "The National Standard Gas Prover of the IMGC-CNR", in Proceedings of the 10th Flomeko Conference, Salvador (Brazil), 5-9 June, 2000

[2] H. Bellinga, F.J. Delhez "Experience with a high-capacity piston prover as a primary standard for high-pressure gas flow measurement", 1993, Flow Measurement and Instrumentation, 4(2): 85-89.

[3] R.F. Berg, T. Gooding, R.E. Vest "Constant pressure primary flow standard for gas flows from 0.01 cm /min to 100 cm /min (0.007–74 μmol/s)", 2014, Flow Measurement and Instrumentation, 35: 84-91.

[4] M.P. van der Beek, R. van der Brink "Gas Oil Piston Prover, primary reference values for Gas-Volume", 2015, Flow Measurement and Instrumentation, 44: 27-33.

[5] Z.P. Xu, J.Y: Dai, H.Y. Chen, D.L. Xie "Development of a reciprocating double-pistons gas prover", 2014, Flow Measurement and Instrumentation, 38: 116-120.

[6] Anonymous, 2009, Details omitted for double-anonymized reviewing

[7] Anonymous, 2010, Details omitted for double-anonymized reviewing

[8] Anonymous, 2019, Details omitted for double-anonymized reviewing

[9] Anonymous, 2019, Details omitted for double-anonymized reviewing

[10] BIPM, IEC, IFCC, ILAC, ISO, IUPAC, IUPAP, and OIML. Evaluation of measurement data — Guide to the expression of uncertainty in measurement. Joint Committee for Guides in Metrology, JCGM 100:2008.

[11] Anonymous, 2020, Details omitted for double-anonymized reviewing

[12] https://emtoolbox.nist.gov/Wavelength/Equation2.asp

[13] https://physics.nist.gov/cuu/Constants/bibliography.html

[14] Meija, Juris, Coplen, Tyler B., Berglund, Michael, Brand, Willi A., De Bièvre, Paul, Gröning, Manfred, Holden, Norman E., Irrgeher, Johanna, Loss, Robert D., Walczyk, Thomas and Prohaska, Thomas. "Atomic weights of the elements 2013 (IUPAC Technical Report)" Pure and Applied Chemistry, vol. 88, no. 3, 2016, pp. 265-291. https://doi.org/10.1515/pac-2015-0305

[15] Lemmon, E.W., Bell, I.H., Huber, M.L.and McLinden, M.O. "NIST Standard Reference Database 23: Reference Fluid Thermodynamic and Transport Properties-REFPROP, Version 10.0" , National Institute of Standards and Technology, Standard Reference Data Program, Gaithersburg, 2018.

Declaration of interests

☒ The authors declare that they have no known competing financial interests or personal relationships that could have appeared to influence the work reported in this paper.

☐The authors declare the following financial interests/personal relationships which may be considered as potential competing interests:

Credit Author Statement

All the Authors did provide a contribution in the various phases of the preparation of the paper

Title page

Metrological features of the Large Piston Prover at INRIM

Aline Piccato[a], Marco Bisi[a], Pier Giorgio Spazzini[a], Fabio Bertiglia[a], Gaetano La Piana[a], Emanuele Audrito[a], Marco Santiano[a], Roberto Bellotti[a] and Claudio Francese[a]

[a] Divisione metrologia applicata e ingegneria, Istituto Nazionale di Ricerca Metrologica, strada delle Cacce 91, Torino, Italy

Corresponding author:

Pier Giorgio Spazzini

E-mail: p.spazzini@inrim.it

Mailing address: C/o INRIM - strada delle Cacce, 91 - I10137 Torino, Italy

Office phone: +39 (0)11 3919941